AMERICAN SOCIETY FOR MICROBIOLOGY | Journal of Virology®

VIRUS-CELL INTERACTIONS

G3BP/Rin-Binding Motifs Inserted into Flexible Regions of nsP2 Support RNA Replication of Chikungunya Virus

Sainan Wang,[a] **Andres Merits**[a]

[a]Institute of Technology, University of Tartu, Tartu, Estonia

ABSTRACT Chikungunya virus (CHIKV) is a mosquito-transmitted alphavirus. In infected cells, its positive-sense RNA genome is translated into polyproteins that are subsequently processed into four nonstructural proteins (nsP1 to 4), the virus-encoded subunits of the RNA replicase. However, for RNA replication, interactions between nsPs and host proteins are also needed. These interactions are mostly mediated through the intrinsically disordered C-terminal hypervariable domain (HVD) in nsP3. Duplicate FGDF motifs in the HVD are required for interaction with mammalian RasGAP SH3-binding proteins (G3BPs) and their mosquito homolog Rin; these interactions are crucial for CHIKV RNA replication. In this study, we inactivated G3BP/Rin-binding motifs in the HVD and inserted peptides containing either native or inactivated G3BP/Rin-binding motifs into flexible regions of nsP1, nsP2, or nsP4. Insertion of native motifs into nsP1 or nsP2 but not into the C terminus of nsP4 activated CHIKV RNA replication in human cells in a G3BP-dependent manner. In mosquito cells, activation also resulted from the insertion of inactive motifs after residue 8 or 466 in nsP2; however, the effect was significantly larger when the inserted sequence contained native motifs. Nonetheless, CHIKV mutants harboring mutations in the HVD and containing insertions of native motifs in nsP2 were not viable in mosquito cells. In contrast, mutant genomes containing native motifs after residue 466 or 618 in nsP2 replicated in BHK-21 cells, with the latter mutant forming infectious progeny. Thus, the binding of G3BPs to nsP2 can support CHIKV RNA replication and restore the infectivity of viruses lacking G3BP-binding motifs in the HVD of nsP3.

IMPORTANCE CHIKV is a reemerging alphavirus that has spread throughout more than 60 countries and is the causative agent of chikungunya fever. No approved drugs or vaccines are available for the treatment or prevention of CHIKV infection. CHIKV replication depends on the ability of its replicase proteins to interact with host cell factors, and a better understanding of host cell factor roles in viral infection will increase our understanding of CHIKV RNA replication and provide new strategies for viral infection attenuation. Here, we demonstrate that the motifs required for the binding of host G3BP/Rin proteins remain functional when transferred from their natural location in nsP3 to different replicase proteins and may enable mutant viruses to complete a full replication cycle. To our knowledge, this is the first demonstration of interaction motifs for crucial host factors being successfully transferred from one replicase protein to another subunit of alphavirus replicase.

KEYWORDS G3BP, RNA replication, Rin, alphavirus, chikungunya virus, nsP2, nsP3

Alphaviruses (family *Togaviridae*) have enveloped virions of approximately 70 nm in diameter and positive-sense RNA genomes approximately 12 kb in length. Most alphaviruses are transmitted by arthropod vectors, and many of them are causative agents of human diseases. Chikungunya virus (CHIKV) has caused major disease outbreaks since 2004. CHIKV infection is associated with fever, rash, and acute and/or chronic inflammatory musculoskeletal- and joint-associated syndromes (1).

The alphavirus genome contains two open reading frames (ORFs). The first ORF is

Editor Bryan R.G. Williams, Hudson Institute of Medical Research

Address correspondence to Andres Merits, andres.merits@ut.ee.

The authors declare no conflict of interest.

Received 15 August 2022
Accepted 16 September 2022
Published 13 October 2022

translated from the genomic RNA into nonstructural (ns) polyproteins designated P123 and P1234, which are precursors of four mature ns proteins, nsP1 to 4. Ns polyproteins and nsPs are virus-encoded components of the alphavirus RNA replicase. The replicase leverages an incoming genome to synthesize negative-sense RNA, and subsequently, this RNA becomes a template for the synthesis of new genomic and subgenomic (SG) RNAs. SG RNA corresponds to the 3′ one-third of the alphavirus genome and is the mRNA for translation of structural proteins encoded in the second ORF. These proteins are first translated in the form of polyprotein precursors that are subsequently processed into six mature structural proteins: capsid protein (CP), E3, E2, 6K, transframe (TF) protein, and E1 (2, 3).

All four nsPs have known enzymatic activities, and their 3D structures have been partially or completely resolved (4). NsP4 is an RNA-dependent RNA polymerase (RdRp) (5). The recently resolved 3D structure of the catalytic domain of nsP4 shows right-hand folds with fingers, palm containing the catalytic GDD motif, and thumb domains. Interestingly, the domain contains several flexible regions, including its C-terminal tail consisting of 12 amino acid residues (6). On its own, nsP4 shows poor solubility and very low RdRp activity (7), indicating that other nsPs are needed for highly efficient RNA synthesis. NsP1 serves as a membrane anchor of the replicase complex and has *S*-adenosyl-L-methionine-dependent methyltransferase and m^7GTP transferase activities that are necessary for capping newly synthesized viral genomic and SG RNAs (8). As recently revealed, nsP1 is assembled in a monotopic membrane-associated dodecameric ring; this organization suggests the structural basis for the coupling between membrane binding, oligomerization, and allosteric activation of the capping enzyme. Similar to nsP4, nsP1 also contains flexible regions, including the entire C-terminal tail after residue 474 (9, 10).

NsP2 exhibits multiple enzymatic activities. It functions as an NTPase, RNA triphosphatase, and RNA helicase (11–14). The structural elements required for these activities are located in the N-terminal portion of the protein (15). However, only full-length nsP2 shows RNA helicase activity, indicating functional cross talk between domains located in the N- and C-terminal portions of the protein (11). The C-terminal portion of nsP2 consists of two domains (16) and exhibits papain-like cysteine protease activity crucial for P123 and P1234 processing (17). Cleavage at the nsP3/nsP4 junction (3/4 site) in P1234 results in the generation of P123 and nsP4, which are subunits of short-lived complexes critical for negative-sense RNA synthesis, which typically occurs in the early stages of infection (up to 3 to 4 h postinfection [hpi]) (18). Subsequently, the 1/2 site and, finally, the 2/3 site are cleaved, resulting in a stable replicase complex consisting of four mature nsPs that synthesize new genomic and SG RNAs (19). The execution of multiple activities and the ability to function both with ns polyproteins and as an individual protein require the intrinsic flexibility of nsP2. Indeed, the recently resolved structure of full-length nsP2 revealed that the N- and C-terminal portions of the protein are connected only by a flexible linker region, which is necessary for viral RNA replication (20).

NsP3 consists of three domains. The first two domains, named the macrodomain and alphavirus unique domain (AUD), are structured (21), but the C-terminal hypervariable domain (HVD) is intrinsically disordered (22). The CHIKV macrodomain has ADP-ribose 1″-phosphate phosphatase (23) and ADP-ribosyl hydrolase activities (24). It can bind ADP-ribosyl groups and hydrolyze mono(ADP-ribosyl)ated proteins; both of these activities are important for alphavirus replication and virulence (24–26). The ADP-ribosyl hydrolase activity of the macrodomain has been shown to reduce the ADP ribosylation of host cell RasGAP SH3-binding protein 1 (G3BP1), an important component in stress granules. Therefore, one of the functions of the macrodomain involves controlling the localization of translation initiation factors during alphavirus infection and making them available for a virus by releasing them from stress granules (27). The functions of the AUD are less clearly understood. A mutagenesis analysis of AUD has revealed that AUD is probably a pleiotropic protein domain with multiple functions during CHIKV RNA synthesis (28). The HVD in CHIKV, Sindbis virus (SINV), and Semliki

Forest virus (SFV) have been shown to be intrinsically disordered, phosphorylated, and capable of interacting with numerous host cell proteins (29–36). Although highly variable, HVDs in alphaviruses contain several conserved short linear interaction motifs. One of these motifs is a duplicate FGDF sequence found in HVDs of Old World alphaviruses. These FGDF motifs bind to the nuclear transport factor 2 (NTF2)-like domain of mammalian G3BP1 and G3BP2 proteins, here collectively called G3BPs (36, 37), as well as to Rin (Rasputin), the mosquito homolog of G3BPs (38). Mutating one FGDF motif in CHIKV nsP3 had no effect on its colocalization with G3BPs or Rin; however, colocalization with G3BPs was lost when both FGDF motifs were mutated (38). The G3BP/nsP3 interaction facilitates alphavirus replication by sequestering G3BP and blocking stress granule assembly; under normal conditions, stress granules stall host and viral protein translation (27, 39, 40). FGDF motifs are required for efficient virus transmission from infected mosquitoes to vertebrate hosts (41). Even more importantly, binding of G3BPs to FGDF motifs is essential for RNA replication of Old World alphaviruses; for CHIKV, this interaction is a clear requirement for viral infection. In this respect, G3BP1 and G3BP2 are, at least partially, redundant: in contrast to the deletion of only one G3BP, knocking out both G3BP genes makes murine cells incapable of supporting CHIKV replication (36). To date, G3BPs (or Rin) remain the only known host cell proteins for which interaction is a requirement for wild-type CHIKV replication (22, 30). Furthermore, the lack of CHIKV replication in the absence of G3BPs is caused by the absence of negative-sense RNA synthesis. The degree to which a lack of G3BPs affects RNA replication varies among different Old World alphaviruses and their strains. Extreme sensitivity to G3BP depletion was found to be linked to an arginine residue at the P4 position of the 1/2 site; replacement of this residue with a histidine residue resulted in partial recovery of CHIKV replication in G3BP knockout cells (42).

The data obtained to date have unequivocally demonstrated that G3BP-binding motifs are crucial for CHIKV RNA replication. However, because at least one additional region in the ns polyproteins is involved in the acquisition of the G3BP depletion-sensitive CHIKV phenotype, CHIKV RNA replication could also be supported by the binding of G3BPs to other ns proteins. Here, we investigated whether replication of CHIKV lacking G3BP-binding motifs in its natural location (i.e., in the HVD of nsP3) can be rescued by adding a 27 amino acid peptide containing two FDGF motifs (the wildtype [WT] peptide) or two mutant AGDF motifs (an F3A peptide) into flexible regions of other nsPs. The results showed that the F3A mutant peptide in the C terminus of the flexible tail of nsP4 inhibited RNA replication in human and mosquito cells and that the negative effect caused by the insertion of the WT peptide was even greater. Adding either of these peptides after amino acid 516 of nsP1 did not rescue RNA replication in mosquito cells. In human cells, a reduction in replicase activity was observed, but the negative effect was significantly less pronounced when the WT peptide was inserted. Insertion of the F3A peptide in the N terminus of nsP2 (after amino acid 8) resulted in strong activation in mosquito but not in human cells; in both cell types, RNA replicase activities were significantly higher when the WT peptide was inserted. The phenotypes acquired by insertion of these peptides after amino acid residues 466 or 618 in nsP2 were similar in both human and mosquito cells; a prominent and significant increase in RNA replication and transcription was also observed when WT peptides were inserted. Finally, we confirmed that in mammalian cells, the insertion of the WT peptide after amino acid residue 466 or 618 in nsP2 restored replication and transcription of the viral genome harboring mutant AGDF motifs in the HVD of nsP3. However, either the release of progeny virions was not observed (with peptide insertion after residue 466) or the mutant virus was strongly attenuated (with peptide insertion after residue 618). Nevertheless, for the first time, our data revealed that the binding sites of crucial host factors can be successfully transferred from their natural location to another alphavirus replicase protein. This finding opens new possibilities for studying multiple roles of G3BPs in alphavirus infection as well as for rational attenuation of alphaviruses.

RESULTS

Insertion of peptides with wild-type or mutant G3BP/Rin-binding motifs into nsP2 increases the activity of mutant CHIKV replicase in mosquito cells. Two natural binding sites of G3BP/Rin are located in the C terminus of the disordered HVD in nsP3 of CHIKV. Mutation of the FGDF motifs to AGDF (the F3A mutation) abolishes negative-sense RNA synthesis and CHIKV replication, demonstrating that binding of these host proteins is crucial for the virus (42, 43). To analyze whether the defect caused by the F3A mutation in nsP3 can be compensated by the insertion of nsP3-derived peptides harboring G3BP/Rin-binding motifs into flexible regions of other ns proteins, a highly sensitive CHIKV *trans*-replicase system was used. In this system, CHIKV ns proteins are expressed by an expression plasmid, while replication-competent template RNA is generated from another plasmid by RNA polymerase I. In the template RNA, the coding region of P1234, with the exception of the first 77 codons that overlap the region containing RNA structures required for virus replication (44), is replaced with a sequence encoding firefly luciferase (Fluc), and the entire structural ORF is replaced by that of *Gaussia* luciferase (Gluc) (Fig. 1A). In this system, the increase in Fluc activity in the presence of an active CHIKV RNA replicase serves as a proxy for full-length ("genomic") template RNA synthesis ("replication"), while an increase in Gluc activity serves as a proxy for SG RNA synthesis ("transcription"). The system has been shown to be efficient in different mammalian cells and, with somewhat lower sensitivity, in mosquito cells (45). We also previously found that after the insertion of enhanced green fluorescent protein (EGFP) after residue 516 in nsP1 or after residue 466 or 618 in nsP2 of CHIKV, these proteins remain functional and maintain their characteristic subcellular localizations (46). Similarly, fusion of a tag consisting of 36 amino acid residues to the flexible C terminus in nsP4 of CHIKV was well tolerated (46), and nsP2 in SINV had been previously shown to tolerate insertion of EGFP after residue 8 (47). Therefore, these sites were selected for the insertion of peptides containing 27 residues derived either from wild-type CHIKV (here designated the WT insertion, sequence, mutant, or peptide) or from 3^{F3A}CHIKV, a construct lacking functional G3BP/Rin-binding sites in nsP3 (here designated the F3A insertion, sequence, mutant, or peptide).

These F3A and WT sequences were first inserted into the Ubi-$P123^{F3A}4$ plasmid designed for P1234 expression, where G3BP/Rin-binding sites in the HVD of nsP3 were inactivated (Fig. 1A). In transfected *Aedes albopictus* C6/36 cells, all obtained plasmids expressed nsP1 at a level similar to that observed for Ubi-P1234. The presence of an insertion in nsP1 was clearly detectable by the slower electrophoretic mobility of the corresponding proteins (Fig. 1B). The insertion of a peptide after residue 8 of nsP2 had no impact on nsP1 levels but reduced the levels of mature nsP2 and nsP3. This outcome was a result of slowed 2/3 site processing; it was confirmed by the detection of unprocessed P23 precursor by antibodies against nsP2 and nsP3 (Fig. 1C and D). This result was consistent with our previous finding showing that the N terminus of nsP2 is important for processing the 2/3 site (48). No difference between proteins containing WT or F3A peptides was observed for any of the pairs (Fig. 1B to D), indicating that the mutations in the F3A peptide exerted no detectable impact on ns polyprotein expression or processing.

To analyze the impact of the introduced mutations on CHIKV RNA synthesis, C6/36 cells were cotransfected with an AlbPolI-Fluc-Gluc template-expressing plasmid and different replicase-expressing plasmids. As we had previously found that an increase in Fluc activity does not reliably reflect the activation of genomic RNA synthesis in these cells (49), we measured and compared only Gluc activity. As expected, the replicase expressed by Ubi-P1234 was highly active, while the activity of replicase in Ubi-$P123^{F3A}4$-transfected cells was at the background level (Fig. 1E). Insertion of any peptide into nsP1 or to the C terminus in nsP4 failed to increase the activity of the mutant replicase, indicating that binding of Rin to these proteins in C6/36 cells did not compensate for the inability of nsP3 to bind the host protein. In contrast, compensation was observed when the WT peptide was inserted after residue 618 in nsP2. At this

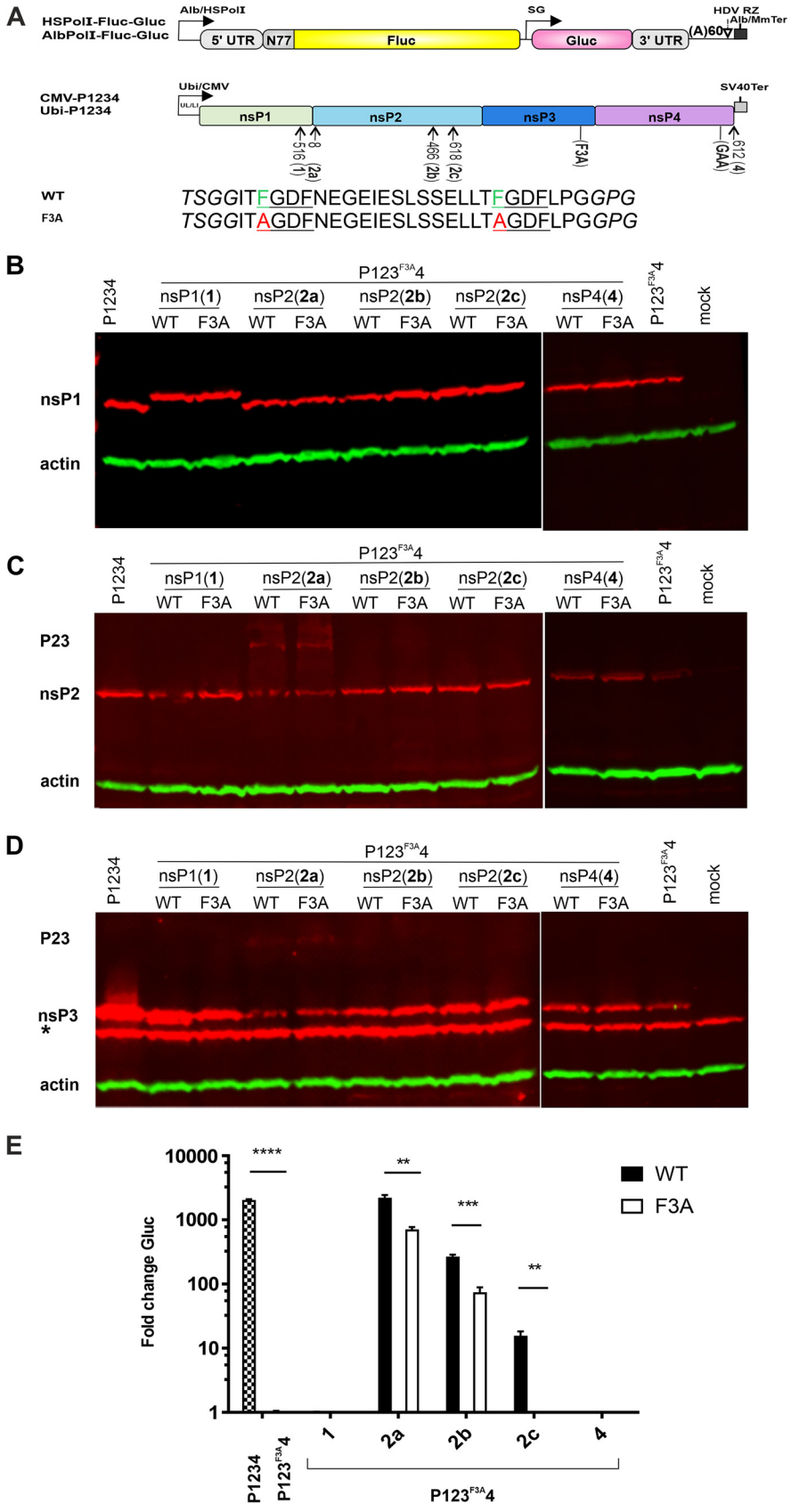

FIG 1 Insertion of WT or F3A peptide into the nsP2 region activates a CHIKV *trans*-replicase lacking G3BP/Rin-binding motifs in the HVD of nsP3 in C6/36 cells. (A) Schematic presentation of the CHIKV

(Continued on next page)

location, although insertion of the F3A peptide caused no increase in RNA replicase activity, insertion of the WT peptide resulted in a clear, approximately 20-fold increase in RNA replicase activity (Fig. 1E). Interestingly, insertion of the F3A peptide after residue 8 in nsP2 prominently increased replicase activity. Importantly, however, the increase in replicase activity resulting from the insertion of the WT peptide was approximately 4-fold higher, clearly indicating that binding of Rin to this location of nsP2 is favorable for the activity of the CHIKV RNA replicase. A similar trend was observed when a peptide was inserted after residue 466. In this case, the insertion of the F3A peptide increased the activity of the mutant replicase approximately 60-fold. As with the other insertion locations in nsP2, a replicase harboring the WT peptide significantly (approximately 5-fold) outperformed its counterpart with the F3A peptide (Fig. 1E). In summary, in C6/36 cells the inability of nsP3 to bind Rin was compensated for by the presence of Rin-binding peptide inserted into different locations in nsP2; the specific effect originating from the ability of the inserted peptide to bind Rin was largest for the insertion after residue 618.

Insertion of the WT peptide into nsP1 or nsP2 increases the activity of mutant CHIKV RNA replicase in human cells. To determine the effect caused by WT or F3A peptide insertion into mutant CHIKV replicase in human cells, peptides were inserted into the aforementioned positions of the CMV-P123^{F3A}4 vector (Fig. 1A). Western blot analysis revealed that the expression of CHIKV ns proteins in transfected human osteosarcoma (U2OS) cells was similar to that observed in C6/36 cells (Fig. 2A to C), except that the constructs harboring insertions after residue 8 in nsP2 expressed higher levels of P23 polyprotein than had been observed in C6/36 cells and that P23 could also be detected in cells transfected with constructs harboring peptide insertions after residue 618 in nsP2 (compare Fig. 1C and D and Fig. 2B and C). These data may indicate a more prominent effect of inserted peptides on ns polyprotein processing in U2OS cells due to different cellular environments and/or higher temperatures that are not optimal for nsP2 protease activity (50). For some constructs, small amounts of products with lower molecular mass and unknown origin were also observed (Fig. 2B and C).

In U2OS cells, wild-type CHIKV replicase efficiently increased the expression of both replication (Fluc) and transcription (Gluc) markers (45), enabling the analysis of the impact of peptide insertion on both replication and transcription. As expected, the F3A mutation in the HVD of nsP3 greatly reduced both replication and transcription (Fig. 2D). In contrast to the effect in C6/36 cells, in U2OS cells insertion of the F3A peptide

FIG 1 Legend (Continued)
trans-replicase system. In CHIKV RNA template expression plasmids AlbPolI-Fluc-Gluc and HSPolI-Fluc-Gluc: Alb/HSPolI, truncated promoter for *Aedes albopictus* or human RNA polymerase I; 5′ untranslated region (UTR), CHIKV 5′ untranslated region, N77, the region encoding the 77 N-terminal amino acid residues of CHIKV nsP1; SG, CHIKV subgenomic RNA promoter; 3′ UTR, truncated CHIKV 3′ untranslated region; HDV RZ, antisense-strand ribozyme of the hepatitis delta virus; Alb/MmTer, terminator of RNA polymerase I in *Aedes albopictus* or mice. In replicase expression plasmids Ubi-P1234 and CMV-P1234: Ubi, full-length *Aedes aegypti* polyubiquitin promoter; UL, transcribed leader of polyubiquitin genes containing a naturally occurring intron; CMV, human cytomegalovirus immediate early promoter; L1, leader region in the herpes simplex virus thymidine kinase gene with an artificial intron; SV40Ter, simian virus 40 late polyadenylation region. F3A designates mutations preventing the binding of G3BP/Rin to the HVD in nsP3, and GAA designates a position with a GDD-to-GAA mutation in the catalytic site in nsP4. The arrows indicate positions where a WT or F3A peptide was inserted into nsP1, nsP2, and nsP4. Amino acid sequences of peptides are provided under the drawing; flexible linker residues are shown in italics; WT or mutant G3BP/Rin-binding motifs are underlined with WT (F) and mutant (A) residues shown in color. (B to D) Expression of CHIKV nsP1 (B), nsP2 (C), and nsP3 (D) in C6/36 cells transfected with different replicase expression plasmids. Cells were collected 48 hpt and lysed, and the obtained samples were analyzed using Western blotting. β-actin was used as the loading control. Positions of CHIKV nsP1, nsP2, nsP3, and P23 are shown; The asterisk (*) indicates mosquito protein recognized by an anti-nsP3 antibody. (E) C6/36 cells were cotransfected with AlbPolI-Fluc-Gluc and Ubi-P1234 (P1234), Ubi-P123^{F3A}4 (P123^{F3A}4), or its variants containing insertions encoding the WT or F3A peptide. Control cells were cotransfected with AlbPolI-Fluc-Gluc and Ubi-P1234^{GAA}. Cells were lysed 48 hpt, and the activities of Gluc (a marker of transcription) were measured and normalized to those of the P1234^{GAA} control (equal to 1; values below that of the control are also shown as 1). Each column represents an average based on three independent experiments; error bars represent the standard deviation. **, $P < 0.01$; ***, $P < 0.001$; ****, $P < 0.0001$ (Student's unpaired *t* test).

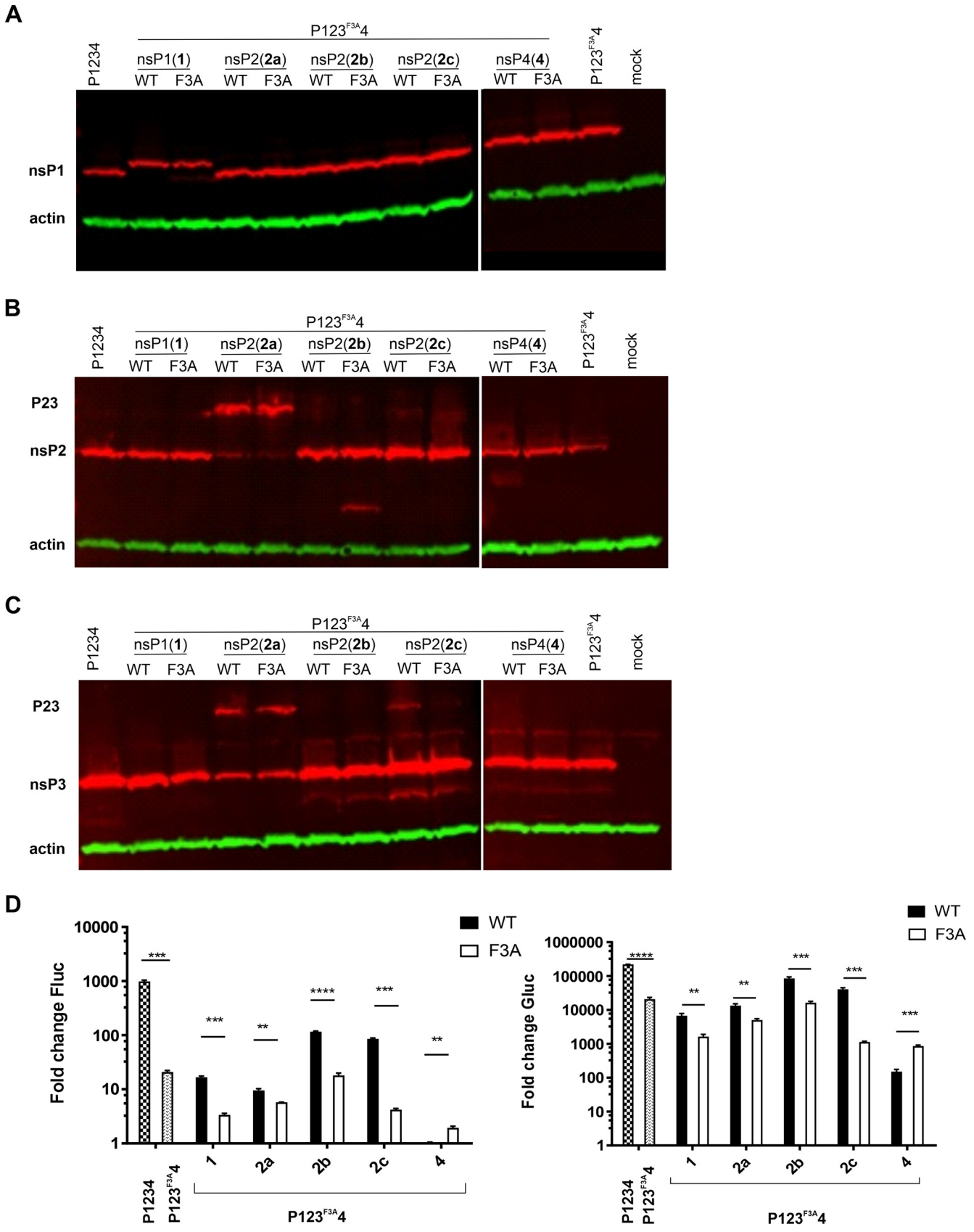

FIG 2 Insertion of WT peptide into nsP1 or nsP2 activates CHIKV *trans*-replicase lacking G3BP/Rin-binding motifs in the HVD of nsP3 in U2OS cells. (A to C) Expression of CHIKV nsP1 (A), nsP2 (B), and nsP3 (D) in U2OS cells transfected with different replicase expression plasmids. Cells were collected 18 hpt,

(Continued on next page)

consistently led to further reduction in the activities of replicases harboring the F3A mutation in nsP3. The degree of this additional reduction differed for different insertion sites, and it was lowest for insertion after residue 466 in nsP2 and largest for fusion with the C terminus in nsP4 (Fig. 2D). The mutant replicases harboring the WT peptide in nsP1 or nsP2 were significantly more active than their counterparts containing the F3A peptide. Similar to the situation in C6/36 cells, the difference was the greatest for peptide inserted after residue 618 of nsP2, with the replicase harboring WT peptide outperforming the replicase with F3A peptide approximately 20-fold for replication (Fluc) and 30-fold for transcription (Gluc). For other locations in nsP2 and nsP1, the observed differences in both replication and transcription were approximately 5-fold and highly significant (Fig. 2D). Surprisingly, however, the opposite outcomes were observed for constructs in which peptides were fused with the C terminus of nsP4. In this case, the active G3BP-binding sites in a fused peptide caused a significant additional reduction in template RNA replication and transcription (Fig. 2D). In summary, in U2OS cells the defect caused by an inability of nsP3 to bind G3BPs was attenuated by insertion of a G3BP-binding peptide into nsP1 or nsP2 but not to the C terminus of nsP4.

FGDF motifs inserted into nsP2 affect CHIKV replicase activity in a G3BP/Rin-dependent manner. Different effects caused by insertion of WT or F3A peptide into nsP2 may originate from the basic properties of the inserted peptides or/and from their ability/inability to bind G3BP/Rin. In CHIKV-infected cells, nsP2 colocalizes with G3BP2 (51), and G3BPs have also been detected in nsP2-specific complexes isolated from SINV-infected cells (47). However, in both of these cases, the interaction of nsP2 with G3BPs may be indirect, i.e., mediated by other component(s) of replicase complexes. Therefore, in this study the interaction with G3BP/Rin was analyzed using plasmids expressing individual nsP2 proteins or their mutant variants rather than plasmids expressing P1234. In transfected U2OS cells, wild-type nsP2 as well nsP2 mutants with F3A or WT peptide inserted after residue 618 colocalized with G3BP1 (Fig. 3A). Although the colocalization signal was strongest for the nsP2 containing WT peptide, the performed quantification showed that the differences from colocalization signals measured for other forms of nsP2 were not significant (data not shown). These data indicate that either an individual nsP2 interacts with G3BPs or that the observed colocalization was a consequence of both proteins being abundant and having similar diffused cytosolic localization (Fig. 3A). To distinguish between these possibilities, the ability of nsP2 harboring the WT or F3A peptide to bind G3BP1/Rin was analyzed using pulldown experiments. The experiments were performed using transfected U2OS and C6/36 cells. EGFP fused to the HVD of nsP3 in CHIKV (33) was the positive control, and EGFP fused to CHIKV nsP2 lacking an inserted peptide was the negative control. In the case of C6/36 cells, the cells were cotransfected with Ubi-AlbRin-V5 plasmid expressing *Aedes albopictus* Rin harboring the V5 epitope tag; this was needed for the detection of Rin (52), as the antibody against the protein itself was not available. As expected, G3BP1/Rin was pulled down by the positive control but not by the negative control, indicating the lack of a direct interaction between nsP2 of CHIKV and G3BP1/Rin. Importantly, pull down of G3BP1/Rin was observed for all three variants of nsP2 harboring the WT peptide but not for their counterparts harboring the F3A peptide (Fig. 3B). These data clearly demonstrate that regardless of its location in nsP2, the WT peptide was able to interact with G3BP1/Rin.

The ability of nsP2 with the inserted WT peptide to interact with G3BP1 does not necessarily mean that it was this interaction that was critical for the increase in RNA

FIG 2 Legend (Continued)
lysed, and analyzed using Western blotting. β-actin was used as the loading control. Positions of CHIKV nsP1, nsP2, nsP3, and P23 are shown. (D) U2OS cells were cotransfected with HSPoll-Fluc-Gluc and CMV-P1234 (P1234), CMV-P123^{F3A}4 (P123^{F3A}4), or its variants containing an insertion encoding the WT or F3A peptide. Control cells were cotransfected with HSPoll-Fluc-Gluc and CMV-P1234^{GAA}. Cells were lysed 18 hpt, and the activities of Fluc (a marker of replication, left panel) and Gluc (a marker of transcription, right panel) were measured and normalized to those of the P1234^{GAA} controls (equal to 1; values below those of control are also shown as 1). Each column represents an average based on three independent experiments; error bars represent the standard deviation. **, $P < 0.01$; ***, $P < 0.001$; ****, $P < 0.0001$ (Student's unpaired *t* test).

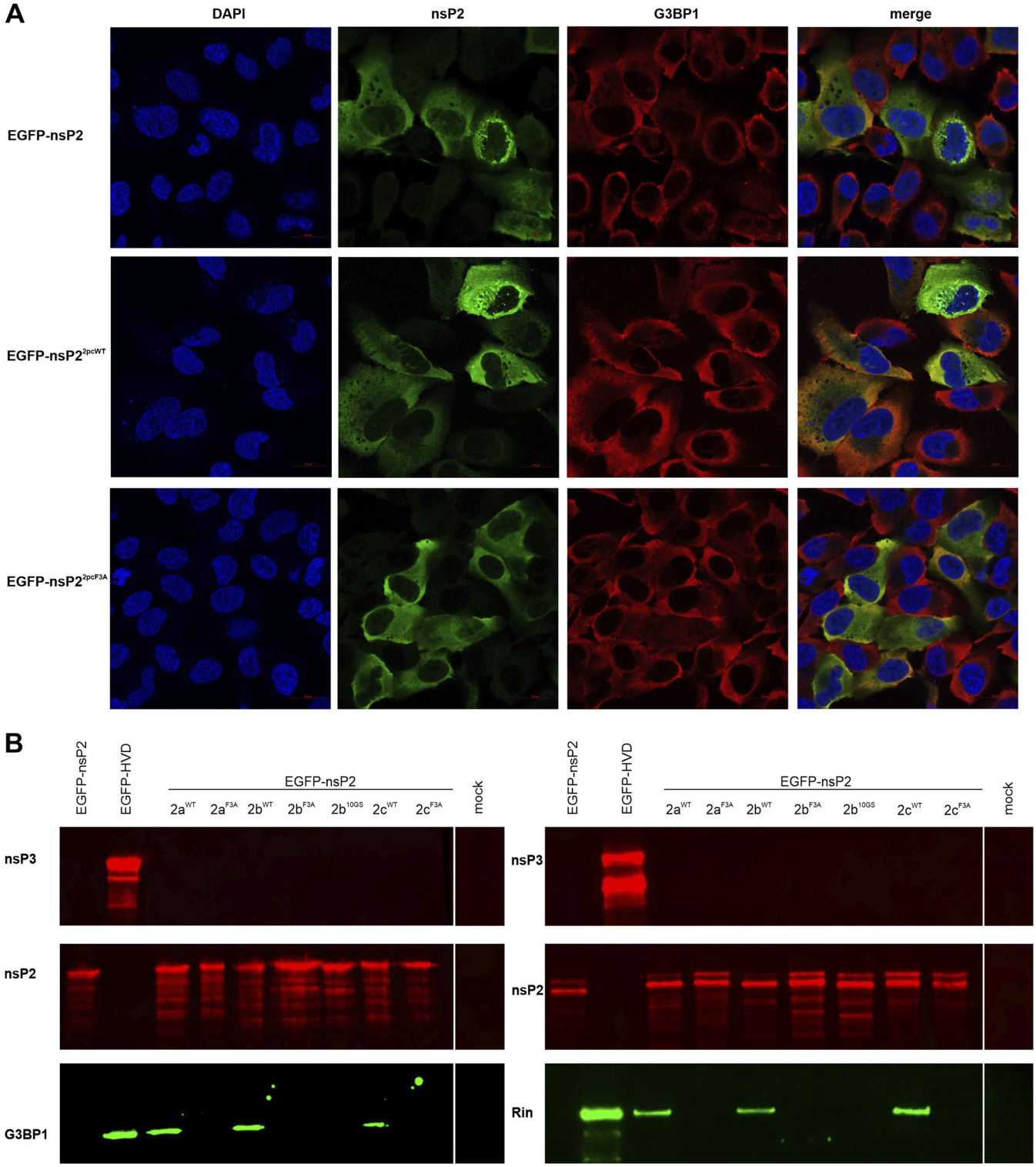

FIG 3 G3BP1/Rin binds to nsP2 containing the WT peptide but not the F3A peptide. (A) U2OS cells were transfected with CMV-EGFP-nsP2, CMV-EGFP-nsP2^{pcWT}, or CMV-EGFP-nsP2^{pcF3A}. Cells were fixed at 24 hpt and immunostained for G3BP1 and CHIKV nsP2. Scale bar = 20 μm. (B) (left) U2OS cells were transfected with CMV-EGFP-nsP2, CMV-EGFP-HVD, CMV-EGFP-nsP2^{paWT}, CMV-EGFP-nsP2^{paF3A}, CMV-EGFP-nsP2^{pbWT}, CMV-EGFP-nsP2^{pbF3A}, CMV-EGFP-nsP2^{pb10GS}, CMV-EGFP-nsP2^{pcWT}, or CMV-EGFP-nsP2^{pcF3A} or mock-transfected; (right) C6/36 cells were cotransfected with Ubi-AlbRin-V5 and Ubi-EGFP-nsP2, Ubi-EGFP-HVD, Ubi-EGFP-nsP2^{paWT}, Ubi-EGFP-nsP2^{paF3A}, Ubi-EGFP-nsP2^{pbWT}, Ubi-EGFP-nsP2^{pbF3A}, Ubi-EGFP-nsP2^{pb10GS}, Ubi-EGFP-nsP2^{pcWT}, or Ubi-EGFP-nsP2^{pcF3A}. At 24 hpt, the cells were lysed, and recombinant proteins and the cellular proteins bound to them were pulled down using EGFP-binding magnetic beads. The samples obtained were analyzed by immunoblotting using antibodies against nsP3, nsP2, and G3BP1 (left) or the V5 epitope tag (right).

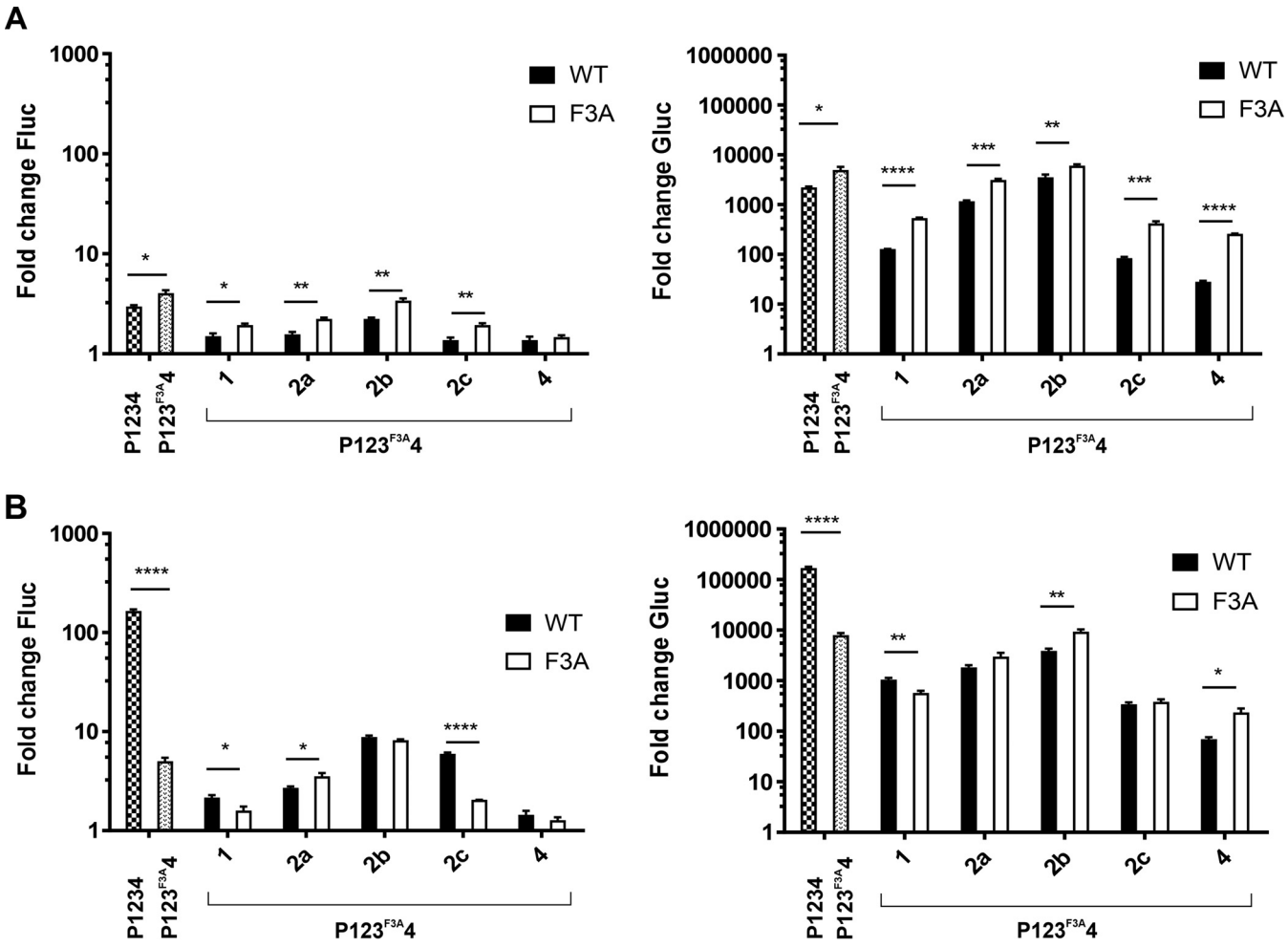

FIG 4 Overexpression of G3BP1 affects the activity of CHIKV *trans*-replicase in U2OS ΔΔ cells. U2OS ΔΔ cells were cotransfected with HSPoll-Fluc-Gluc and CMV-P1234 (P1234), CMV-P123^{F3A}4 (P123^{F3A}4) or its variants containing insertions encoding the WT or F3A peptide. Control cells were cotransfected with HSPoll-Fluc-Gluc and CMV-P1234^{GAA}. (A and B) The CMV-G3BP1 plasmid was either not added (A) or added (B) to the transfection mixture. The experiment was performed and the data were collected and analyzed as described in the legend of Fig. 2D. *, $P < 0.05$; **, $P < 0.01$; ***, $P < 0.001$; ****, $P < 0.0001$ (Student's unpaired *t* test).

replication observed in previous experiments (Fig. 1E and 2D). Therefore, U2OS-derived double-null ΔΔG3BP1/2-knockout (KO) cells (U2OS ΔΔ cells) (53) were cotransfected with HSPoll-Fluc-Gluc and a plasmid expressing CHIKV P1234 or its mutant forms. Consistent with previous results (42), only very low replication and greatly reduced transcription rates were observed in the U2OS ΔΔ cells transfected with CMV-P1234 (Fig. 4A). Unexpectedly, in U2OS ΔΔ cells, the replicase harboring the F3A mutation in nsP3 outperformed the wild-type replicase (compare Fig. 2D and 4A). The same observation was made with every pair of mutant replicases harboring WT or F3A peptide insertions; in most cases, the observed differences were significant (Fig. 4A). Considering these findings, we concluded that mutant AGDF motifs in the absence of G3BPs led to higher replication and transcription levels of template RNA regardless of whether the motifs were located in the native position (in the HVD of nsP3) or in the peptides inserted in other ns proteins.

To confirm the importance of the presence of G3BP on the activities of the CHIKV replicase and its mutant versions, we performed the previously mentioned experiment with U2OS ΔΔ cells in the presence of a plasmid expressing G3BP1. The overexpression of G3BP1 in U2OS ΔΔ cells drastically increased the activity of the wild-type CHIKV replicase but had only a negligible positive impact (approximately 1.2-fold for replication and 1.6-fold for transcription; no statistical significance) on the activities of replicase

harboring the F3A mutation in the HVD of nsP3 (compare Fig. 4A and B). Similarly, overexpression of G3BP1 exerted only a minor effect on the activities of replicases harboring the F3A peptide in nsP1, nsP2, or nsP4. A replicase harboring the WT peptide in nsP4 did benefit little, if at all, from G3BP1 overexpression. In contrast, the replicase harboring the WT peptide in nsP1 became significantly more active than its counterpart harboring the F3A peptide (Fig. 4B). The replication activities of replicases with WT peptide insertions after residue 466 or 618 in nsP2 also became higher than those of their counterparts with F3A peptides; however, the difference was significant only for the replicase harboring an insertion after position 618. The transcriptional activities of replicases with the WT peptide insertion after residue 8 or 618 became similar to those of replicases with the F3A peptide insertion. The transcriptase activity of the replicase with the WT peptide insertion after residue 466 was only slightly increased by G3BP1 overexpression and remained significantly lower than that of the replicase with the inserted F3A peptide (Fig. 4B). Taken together, our data confirm that the WT peptide inserted into nsP2 can bind G3BP1/Rin and that G3BP is required to increase the activity of CHIKV replicases harboring a WT peptide insertion.

Insertion of a flexible linker after residue 466 of nsP2 activates the RNA replicase activity of P123^{F3A}4 in a G3BP-independent manner. In U2OS ΔΔ cells, replicases harboring inserted F3A peptides outperformed their counterparts with WT peptides; this indicates an advantage provided by the former insertion. In the case of insertions after residue 466 of nsP2, this advantage was large enough to be maintained even when cells were cotransfected with the G3BP1 expression plasmid (Fig. 4). A previous study showed that the flexible linker inserted after residue 466 of nsP2 could increase the activity of CHIKV RNA replicase as well as the infectivity of the corresponding virus (20). Therefore, the F3A peptide, harboring smaller Ala residues instead of bulkier Phe residues present in the WT peptide, was hypothesized to also act as a flexible linker. To investigate this possibility, we inserted a linker consisting of 10 flexible amino acid residues (10GS) after residue 466 of nsP2 expressed from CMV-P123^{F3A}4 and CMV/Ubi-EGFP-nsP2 plasmids and performed the set of experiments described above.

The pulldown experiment revealed that nsP2^{pb10GC} was unable to interact with G3BP1/Rin (Fig. 3B), excluding the possibility that any effect caused by this insertion may be due to G3BP binding. In wild-type U2OS cells, the replicase expressed from CMV-P12^{pb10GS}3^{F3A}4 outperformed replicases expressed from CMV-P123^{F3A}4, CMV-P12^{pbWT}3^{F3A}4, and CMV-P12^{pbF3A}3^{F3A}4. The effect was more prominent for replication activity and less pronounced for transcription activity (Fig. 5A). In U2OS ΔΔ cells, the replicase expressed from CMV-P12^{pb10GS}3^{F3A}4 outperformed all other replicases, with the difference being smallest with replicase expressed from CMV-P12^{pbF3A}3^{F3A}4 (Fig. 5B). Predictably, coexpression of G3BP1 allowed the wild-type replicase to outperform that expressed from CMV-P12^{pb10GS}3^{F3A}4; however, the latter remained more active than any other mutant replicase used in the experiment (Fig. 5C). Taken together, the obtained data confirm that the flexible linker inserted after residue 466 of nsP2 of the mutant (lacking G3BP binding motifs in nsP3) replicase increased its RNA replicase activity in a G3BP-independent manner. The insertion of the F3A peptide caused a similar (albeit smaller) effect. Therefore, it likely also acted as a flexible linker, and this effect did not depend on the presence of G3BP. The more pronounced effect observed for the 10GS linker was most likely caused by the higher flexibility and/or shorter length of this insertion.

Insertion of a sequence encoding the WT or F3A peptide into the nsP2 region does not restore replication of the SP6-3^{F3A}CHIKV transcript in mosquito cells. The experiments described above revealed that the WT peptide insertion after residue 8, 466, or 618 in nsP2 activated the mutant CHIKV (P123^{F3A}4) *trans*-replicase in C6/36 cells; to a lesser degree, this outcome was observed in replicases with the F3A peptide inserted after residue 8 or 466 in nsP2 (Fig. 1E). The insertion of the WT peptide also allowed binding of G3BP1/Rin to nsP2 (Fig. 3B), and the replication/transcription activities of the corresponding CHIKV *trans*-replicase in U2OS cells were increased in a G3BP-dependent manner (Fig. 4A and B).

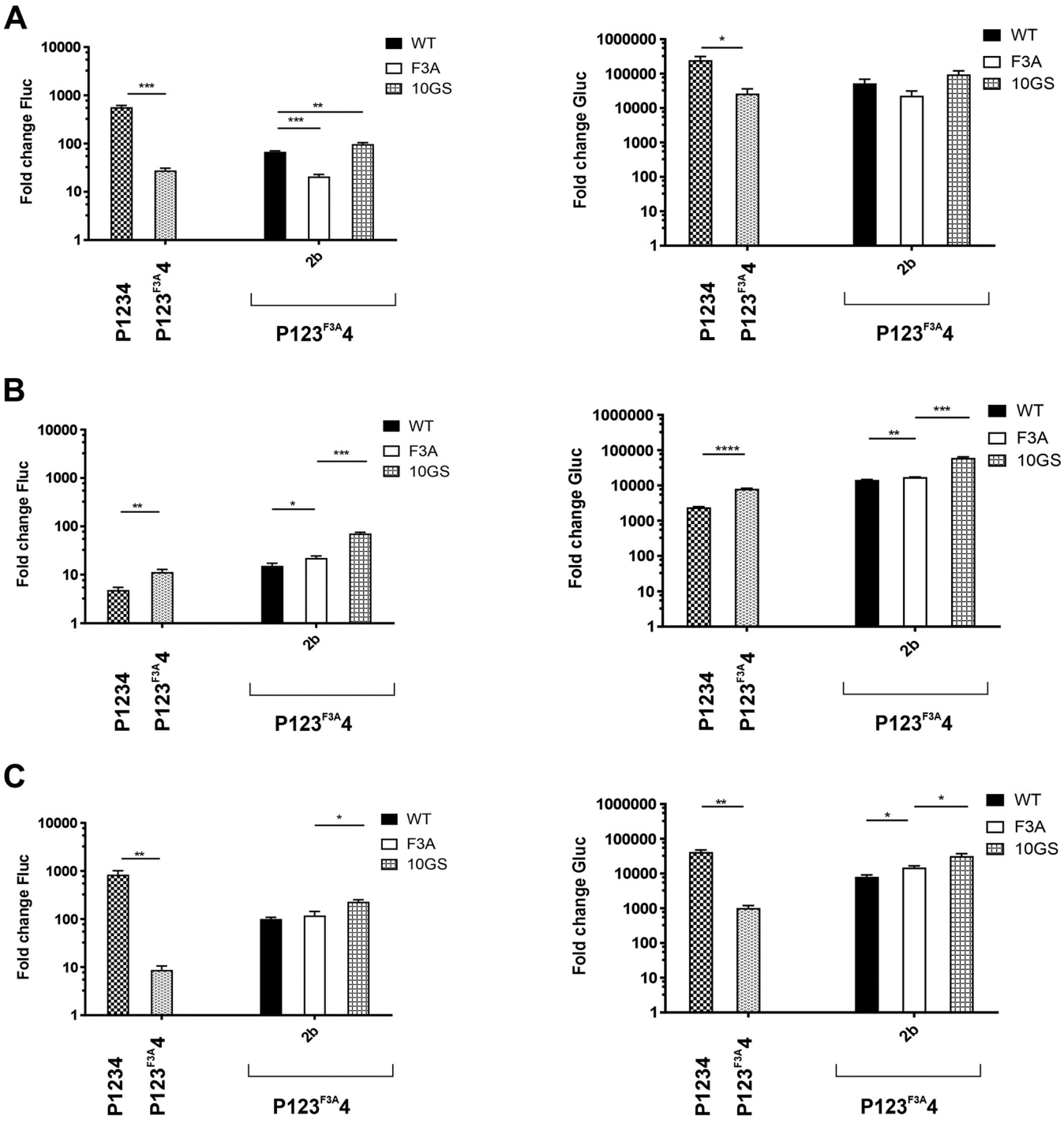

FIG 5 The flexible linker inserted after residue 466 of CHIKV nsP2 increases the RNA replicase activity of CHIKV P123^{F3A}4 in a G3BP-independent manner. (A to C) U2OS (A) or U2OS ΔΔ (B and C) were cotransfected with HSPolI-Fluc-Gluc and CMV-P1234 (P1234), CMV-P123^{F3A}4 (P123^{F3A}4), or its variants containing an insertion encoding the WT peptide, F3A peptide, or 10GS linker after residue 466 of nsP2. Control cells were cotransfected with HSPolI-Fluc-Gluc and CMV-P1234^{GAA}. The CMV-G3BP1 plasmid was either not added (A and B) or added (C) to the transfection mixture. Cells were lysed 18 hpt, and the activities of Fluc (a marker of replication, left panels) and Gluc (a marker of transcription, right panels) were measured and normalized to those of the P1234^{GAA} controls (equal to 1; values below these of the control are also shown as 1). Each column represents an average based on three independent experiments; error bars represent the standard deviation. *, $P < 0.05$; **, $P < 0.01$; ***, $P < 0.001$; ****, $P < 0.0001$ (Student's unpaired *t* test).

To analyze whether the activating effects are also observed in the context of the virus genome, corresponding mutations were introduced into the infectious cDNA (icDNA) clone SP6-CHIKV and its mutant SP6-3^{F3A}CHIKV, harboring the FGDF-to-AGDF substitution mutation in natural G3BP/Rin-binding motifs located in the HVD of nsP3 (42).

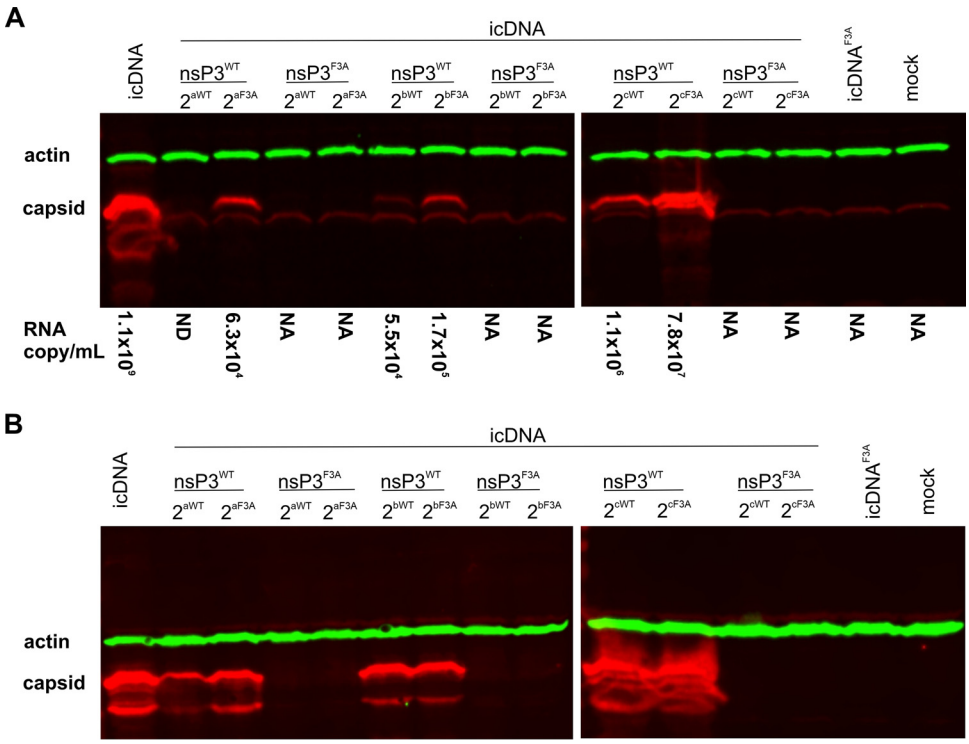

FIG 6 Insertion of the sequence encoding the WT or F3A peptide in the nsP2 region of SP6-3^{F3A}CHIKV does not rescue replication of corresponding transcripts in C6/36 cells. (A) C6/36 cells were transfected with 5 μg of capped RNA transcripts of SP6-CHIKV, SP6-3^{F3A}CHIKV, or their mutants harboring an insertion in the nsP2 region. The transfected cells were incubated at 28°C for 72 h, after which, P_0 virus stocks were collected. The cells were harvested and lysed, and the samples obtained were subjected to SDS-PAGE with 12% gels. The CHIKV capsid protein was detected using the corresponding antibody; an antibody against β-actin was used to detect the loading control. The number of viral RNA copies in selected P_0 stocks was measured using RT-qPCR and is presented below the panel as the RNA copy/mL; ND, not detectable; NA, not analyzed. (B) A total of 150 μL of each obtained P_0 stock was used to infect 1×10^6 BHK-21 cells. The cells were incubated at 37°C until CPEs were observed or for 72 h, collected, and analyzed as described in panel A. The data from one of three independent reproducible experiments are shown.

To analyze the effect of these insertions on viral replication in mosquito cells, C6/36 cells were transfected with capped transcripts of SP6-CHIKV, SP6-3^{F3A}CHIKV, or their mutant variants. CP expression, analyzed using Western blotting, was used as the criterion for successful viral RNA synthesis, as its expression requires replication of incoming RNA transcripts and synthesis of SG RNA. In C6/36 cells transfected with transcripts of SP6-3^{F3A}CHIKV or mutants based on this construct, no expression of CP was observed (Fig. 6A). Furthermore, no CP expression was observed in BHK-21 cells infected using supernatants of the medium harvested from transfected C6/36 cell cultures (Fig. 6B). Thus, in C6/36 cells, the activating effects of peptide insertions into nsP2 observed for the *trans*-replicase (Fig. 1E) were not reproduced in the context of the 3^{F3A}CHIKV RNA genome that remained noninfectious for mosquito cells. In contrast, transcripts of SP6-CHIKV and the mutants based on it were infectious, indicating that the insertion of the peptides *per se* was tolerated. Interestingly, in transfected C6/36 cells, CP expression was consistently lower for viruses harboring the WT peptide insertion than for their counterparts harboring the F3A peptide (Fig. 6A). The effect was most prominent for virus containing the WT peptide insertion after residue 8 in nsP2; in this case, no CP expression was detected in transfected C6/36 cells. Similarly, CP expression was very low for the viruses with the WT peptide insertion after residue 466. This trend was similar to that observed for the activities of mutant CHIKV *trans*-replicases in U2OS $\Delta\Delta$ cells (Fig. 4A) and may indicate that where G3BP/Rin-binding either was not required (as here for viruses with wild-type nsP3) or was impossible (as in U2OS $\Delta\Delta$ cells), insertion

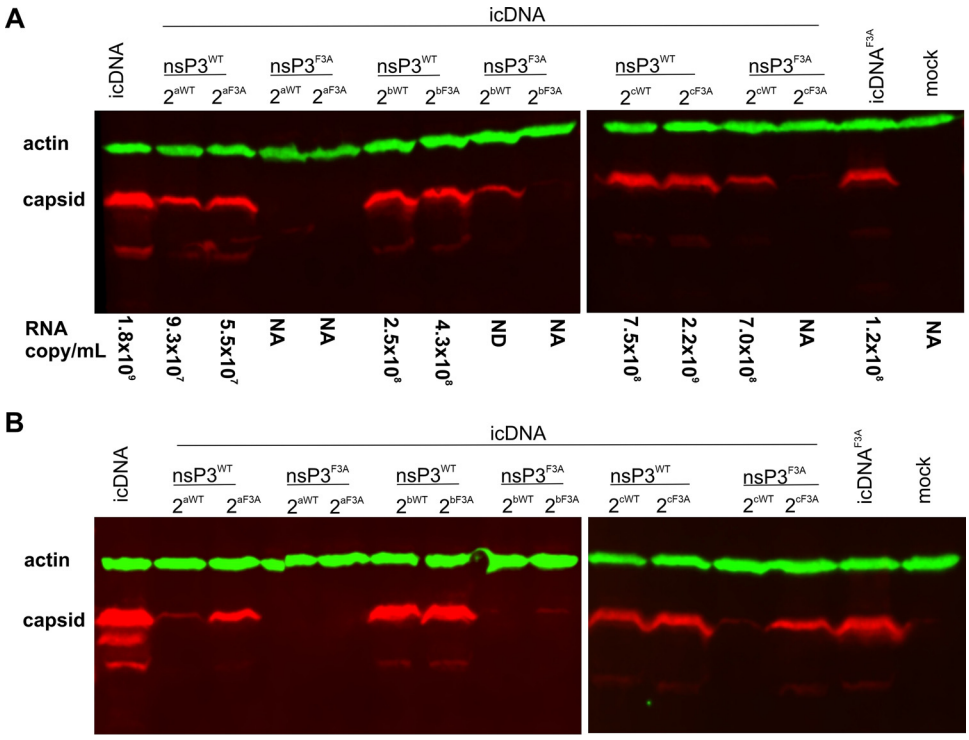

FIG 7 Insertion of the sequence encoding the WT but not the F3A peptide in the nsP2 region of SP6-3^{F3A}CHIKV rescues replication of corresponding transcripts in BHK-21 cells. (A) BHK-21 cells were transfected using 5 μg of capped RNA transcripts of SP6-CHIKV, SP6-3^{F3A}CHIKV, or their mutants harboring an insertion in the nsP2 region. The transfected cells were incubated at 37°C until CPEs were observed or for 72 h, after which, P_0 virus stocks were collected, and cells were harvested. Virus stocks and cell lysates were analyzed, and the data are presented as described in Fig. 6A. (B) A total of 150 μL of each obtained P_0 stock was used to infect 1×10^6 BHK-21 cells. The experiment was performed, and the data are presented as described in Fig. 6B. The data from one of three independent reproducible experiments are shown.

of the F3A peptide was less deleterious to CHIKV than insertion of the WT peptide. These data were confirmed by reverse transcriptase quantitative PCR (RT-qPCR) analysis, which revealed that the number of viral RNA genome copies in harvested supernatants was consistently lower for viruses harboring the WT peptide in nsP2 (Fig. 6A). However, when collected P_0 stocks were used to infect BHK-21 cells, CP expression was observed in cells harboring each of the mutants; however, the level was again lowest in cells with the virus harboring the WT peptide insertion after residue 8 in nsP2 (Fig. 6B). Most likely, these data indicate that in BHK-21 cells the defects caused by insertion of the WT peptide were less severe than those in C6/36 cells and may not be observed for all three insertion sites.

Insertion of the sequence encoding the WT peptide after residue 466 or 618 in nsP2 restores the infectivity of the SP6-3^{F3A}CHIKV transcript in BHK-21 cells. BHK-21 cells were transfected with RNA transcripts of icDNAs of WT CHIKV, 3^{F3A}CHIKV, or their mutants and analyzed as described above. In contrast to C6/36 cells, no clear difference between mutants based on WT CHIKV harboring either the WT or F3A insertion was observed (Fig. 7A). The viruses with WT or F3A peptide insertion after residue 466 or 618 in nsP2 also showed similar CP expression levels in BHK-21 cells infected with P_0 stock, confirming that, for these mutants, the negative impact of WT peptide insertion observed in the C6/36 cells was a cell-type-specific effect. In contrast, for viruses harboring an insert after residue 8 in nsP2, the WT peptide was associated with lower CP expression levels in infected BHK-21 cells (Fig. 7B) and the absence of cytopathic effects (CPE), indicating that the virus was also attenuated in BHK-21 cells.

Development of CPEs and high levels of CP expression were also observed for BHK-21 cells transfected with RNAs of 3^{F3A}CHIKV that were used as a negative control. The

genome copy number in the harvested supernatant was high, and the virus present in the supernatant was capable of successfully infecting BHK-21 cells (Fig. 7A and B). Previously, we observed that 3^{F3A}CHIKV recovered infectivity by deleting a fragment of mutated HVD in nsP3 in a manner that reestablished one of the G3BP-binding motifs (42). To analyze whether the same mechanism led to the outcome in this experiment, sequences of regions corresponding to those of the HVD of nsP3 and to the nsP1-nsP2 junction, which had been shown to be associated with the ability of CHIKV to grow in the absence of G3BP binding (42), were analyzed. Sequencing of five independent clones corresponding to the HVD in nsP3 failed to reveal a previously observed deletion. However, all of the clones contained different mutations, including deletion of amino acid residues 429 to 514 (which removed both mutated G3BP motifs), residues 331 to 493 (which removed the first mutated G3BP motif), or residues 504 to 514 in nsP3. None of these mutations restored G3BP-binding sites, and their roles in the restoration of 3^{F3A}CHIKV infectivity remain unclear. Sequencing of the clones corresponding to the nsP1-nsP2 junction revealed an Arg532, a P4 residue of the 1/2 site, substituted with a glycine in one of five clones. As an Arg532-to-histidine substitution had been previously shown to allow replication of CHIKV harboring the F3A mutation in the HVD of nsP3 (42), the Arg532- to-glycine-substitution was hypothesized to have a similar effect. To verify this hypothesis, these mutations were introduced into CMV-$P123^{F3A}4$, and the activities of the obtained replicases were analyzed in U2OS cells. Introduction of Arg532His or Arg532Gly substitution resulted in an approximately 8-fold ($P < 0.0001$ for both substitutions) increase in replication activity. An increase in transcriptional activity was also observed, but the effect was smaller (approximately 1.4-fold) and not significant ($P = 0.285$) for the Arg532Gly substitution and somewhat large (approximately 2.7-fold) and significant ($P < 0.05$) for the Arg532His substitution. In summary, various mutations in the nsP1-nsP2 junction and/or the HVD in nsP3 were found in the progeny of 3^{F3A}CHIKV. The Arg532Gly substitution was confirmed to act as a compensatory mutation; although the effects of the mutations found in nsP3 were not characterized in detail, the construct presumably reacquired infectivity through the accumulation of different second-site mutations located in regions known to affect the sensitivity of CHIKV for the lack of the nsP3/G3BP interaction (42).

No CP expression or infectious progeny was observed for 3^{F3A}CHIKV mutants with the WT or F3A insertion after residue 8 in nsP2 (Fig. 7A and B). In contrast, clear differences between 3^{F3A}CHIKV mutants harboring the WT or F3A insertion after residue 466 or 618 in nsP2 were detected. No CP expression was observed in BHK-21 cells transfected with RNAs from icDNAs harboring the inserted F3A sequence. In sharp contrast, CP expression was observed for constructs harboring the WT peptide insertion. Interestingly, only a virus with a WT peptide insertion after residue 618 in nsP2 released a high level of RNA genomes, presumably packaged into virions, into the growth medium (Fig. 7A). For constructs with the WT peptide insertion after residue 466, the number of released genome copies was below the detection level, indicating that the WT peptide in this position restored viral RNA replication and transcription but had a negative impact on virion formation and/or release. Consistently, no CP expression was observed in BHK-21 cells infected with the corresponding supernatant (Fig. 7B). In contrast, low but clearly detectable levels of CP expression were observed for BHK-21 cells infected with supernatants containing virus harboring the WT peptide after residue 618 in nsP2 (Fig. 7B). The virus was, however, strongly attenuated and did not cause a CPE in transfected or infected cells. Reverse transcriptase PCR (RT-PCR) and sequencing analysis confirmed the absence of adaptive mutations in the 1/2 site and HVD of these viruses. Thus, the restored infectivity was due to WT peptide insertion. These properties contrasted with the negative control that acquired second-site compensatory mutations and restored the cytopathogenic phenotype. High levels of CP expression (Fig. 7B) and strong CPEs were also observed in BHK-21 cells infected with progeny of the construct harboring the F3A peptide inserted after residue 618 in nsP2. Similar to the progeny of 3^{F3A}CHIKV, the Arg532-to-glycine mutation was detected in

the P_1 stock of this virus. Low levels of CP expression were observed for progeny of the construct harboring the F3A peptide after residue 466 in nsP2 (Fig. 7B). In this case, the harvested P_1 stocks did not contain sufficient viral RNA for sequence analysis; nevertheless, the observed recovery was highly likely to be due to second-site mutations, as had been found for other constructs lacking G3BP-binding sites and in a previous study (42). Taken together, our data clearly demonstrate that removal of a binding site for the most crucial host factor from one of the replicase proteins of CHIKV can, at least to some degree, be compensated for by the insertion of the binding site for the same factor in a different replicase protein.

DISCUSSION

G3BP1 together with G3BP2 contributes to stress granule formation (54), which plays an important role in cellular reactions to different stresses (55). Stress granules and G3BPs are therefore believed to exert an antiviral effect on alphavirus replication. However, G3BPs (Rin in mosquito cells) are important proviral host factors for CHIKV and other Old World alphaviruses (36). Although G3BPs coprecipitate with different replicase proteins of alphaviruses (47, 56, 57), the NTF2-like domain in G3BPs and FGDF motifs in nsP3 are what directly interact (37, 43). Depletion of G3BPs or mutation of the motifs in nsP3 required for G3BP binding results in similar effects, including inhibition of CHIKV replication and blockade of negative-sense RNA synthesis (36, 42, 51, 58), indicating that CHIKV recruits G3BPs into its replication complex and/or uses it to control some RNA replication-related processes. The multiple roles of G3BPs in CHIKV infection make them the most important known host factor of CHIKV; however, multifunctionality also complicates functional analysis of their exact roles in an infection. In this study, we applied a unique approach consisting of inactivation of G3BP-binding motifs in their native location and insertion of a G3BP-binding peptide or its mutant variant into different ns proteins of CHIKV followed by analysis of the effects of these mutations on CHIKV RNA replicase activities and on replication of mutant viruses.

The effects caused by the insertion of peptides into CHIKV *trans*-replicase lacking G3BP/Rin-binding sites in nsP3 in mosquito and human cells were not identical. First, the replicase with the WT peptide inserted into nsP1 outperformed its counterpart with the F3A peptide in human cells (Fig. 2D); however, in mosquito cells the activities of both of these replicases were at the background level. Considering that the insertion of EGFP into the same position also had a much larger negative effect on the activity of the CHIKV *trans*-replicase in mosquito cells than in human cells (59), the different impacts of WT peptide insertion may reflect a host cell-specific effect. However, as the basic activity of the CHIKV *trans*-replicase lacking G3BP/Rin-binding sites in nsP3 in mosquito cells was very low, we cannot exclude the possibility that the assay used was not sufficiently sensitive to detect differences between these two mutants. Second, in mosquito cells, insertion of the F3A peptide after residue 8 or after residue 466 in nsP2 resulted in a profound increase in the transcriptional activity of the mutant CHIKV *trans*-replicase; in human cells, the same insertions caused a decrease in replicase activity (compare Fig. 1E and 2D). For the replicase with an insertion after residue 8 in nsP2, the impact was likely caused by the delay in processing the 2/3 site (Fig. 1C and D and Fig. 2B and C), as completely blocking the processing of this site boosted CHIKV replicase activity in mosquito cells but not in human cells (59). We previously observed that an insertion of linkers with a length of 6 or 10 amino acid residues after residue 466 in nsP2 of CHIKV had no impact on the transcriptional activity of *trans*-replicase in human cells, but the same insertions did cause a significant (albeit relatively small) increase in transcription in mosquito cells (20). We also observed that in human cells, 6- or 10-amino acid flexible linkers increased the replication activity of the *trans*-replicase. Here, a 10-amino acid flexible linker inserted into nsP2 of the *trans*-replicase lacking G3BP/Rin-binding sites in nsP3 also increased its RNA replicase activities in WT U2OS cells (Fig. 5A). This effect was not observed for the F3A peptide (Fig. 2D and 5A), possibly because of its longer

length (34 amino acid residues) and/or different sequence. In summary, the effects caused by the insertion of the F3A peptide were remarkably consistent with previous observations, increasing confidence in the suggestion that different properties from replicases harboring the WT peptide were indeed due to two phenylalanine-to-alanine substitutions (Fig. 1A) and the ability/inability of the introduced peptide to interact with G3BP/Rin (Fig. 3B).

Interestingly, our data revealed that in the absence of G3BPs (i.e., in U2OS ΔΔ cells), functional motifs for G3BP binding reduced the synthesis of viral RNAs (Fig. 4A). This situation was possibly entirely artificial and/or limited to the substitution of hydrophobic phenylalanine with a neutral alanine residue. However, this result has conceivably broader biological significance, indicating that binding motifs for host factors, if they cannot perform (or are not required for) essential functions, may be harmful to a virus. One possibility is that these motifs may disrupt the interaction between viral ns proteins; however, our data showing that the negative effect does not depend on the replicase protein in which the motif is located argue against this possibility. More likely, different motifs compete with each other, i.e., binding of one cellular factor in one motif affects the binding of another in a different motif. This possible outcome may be caused by steric hindrance and/or altered structure/accessibility of the motifs. Thus, mutant AGDF motifs may allow more efficient binding of other proviral factors that are less important for CHIKV RNA replication than G3BPs. To our knowledge, G3BP-binding motifs do not directly overlap with the binding motifs of other host proteins; the motifs for the binding of NAP1L1 and NAP1L4, which are located near the FGDF motifs (29), for example, were not included with the peptides used in this study (Fig. 1A). The sequence between FGDF motifs has been shown to respond to the binding of SH3 domains in host proteins to binding sites located 100 amino acid residues upstream of the HVD in nsP3 (31). Interestingly, in U2OS ΔΔ cells, differences between replicases harboring the WT and F3A peptide were observed even when the peptides were inserted in nsP1 or nsP2, i.e., in regions that are very unlikely to be affected by the binding of SH3-domain proteins to nsP3 (Fig. 4A). Therefore, the sequence between FGDF motifs likely also affects CHIKV RNA replication in a G3BP- and SH3-domain protein-binding-independent manner. The enhanced negative impact that the insertion of the WT peptide had on CHIKV RNA replicase activity is also one possible reason for the peculiar effect seen for mutant replicases harboring inserted peptides in the C terminus of nsP4. In WT U2OS cells, the WT peptide introduced into this position reduced the activity of the replicase more profoundly than the F3A peptide (Fig. 2D). This outcome may also suggest that the binding of G3BPs to the C terminus of nsP4 could prevent/weaken the interaction of nsP4 with P123 or the products of its processing. This assumption is consistent with very recent data about the molecular architecture of the core of alphavirus replicase: in this structure consisting of 12 molecules of nsP1, 1 molecule of nsP2, and 1 molecule of nsP4, the C terminus of nsP4 is, in fact, also well folded and points to the spherule side of the replicase core (60). Thus, it should be inaccessible for interaction with host proteins, and artificially introduced interaction sites may indeed interfere with replicase complex formation and functioning.

For several positive-sense RNA viruses, short linear interaction motifs that interact with host proteins are clustered together in intrinsically disordered regions in some replicase proteins, for example, in the C terminus of NS5A of hepatitis C virus (61) or in the HVD of nsP3 in alphaviruses (31). The location of motifs in long disordered regions is assumed to be beneficial because it increases the accessibility of motifs to their binding partners and/or allows complex interplay between motifs, their modifiers (such as kinases) and host proteins. In this regard, the WT peptide inserted into short flexible regions of nsP2, not known to contain motifs for binding host proteins, was interestingly capable of activating CHIKV RNA replication in a G3BP/Rin-binding-dependent manner (Fig. 1E and 2D) and, in two cases, even rescued the replication of the 3^{F3A}CHIKV genome in BHK-21 cells (Fig. 7A). Although the rescue of viral activities was

only partial, these data clearly indicate that location in a long intrinsically disordered region is not mandatory for binding motif function.

The results from experiments with the *trans*-replicase system have been repeatedly shown to be correlated with data obtained using mutant viruses (25, 33, 46, 48, 62). However, CHIKV *trans*-replicase is extremely sensitive and may reveal effects that have no relevance to true viruses; for example, replicases harboring lethal mutations may display activity levels greater than the background (17, 45). Similarly, the mandatory in *trans* interaction of template RNA and ns proteins may enhance the impacts of some mutations, and as a result, certain effects, poorly detectable in virus-infected cells, may appear prominently in a *trans*-replication assay (59). Therefore, demonstrating that the effects observed using a *trans*-replication assay can be seen using virus genomes increases the credibility of the findings. Insertion of the WT peptide into selected positions in nsP2 of 3^{F3A}CHIKV did not lead to restoration of the corresponding virus in C6/36 cells (Fig. 6). In contrast, the corresponding *trans*-replicases were active, and for replicases harboring the WT peptide insertion after residue 8 in nsP2, the transcriptional activity in C6/36 cells was similar to that of the original CHIKV replicase (Fig. 1E). The rescue in C6/36 cells may have failed because of insufficient transfection efficiency. Indeed, we observed that the transfection of these cells with plasmid DNA or *in vitro* transcribed RNA was much less efficient than that of BHK-21 cells. However, the failure of the restorative effect could conceivably be based on biological reasons. For example, binding of Rin to the N terminus of nsP2 may interfere with the switch from ns polyprotein translation to RNA replication, an event required during virus rescue and infection but not for the activity of the *trans*-replicase used in this study. This mechanism explains why the rescue of the virus with native nsP3 and the WT peptide inserted after residue 8 in nsP2 of C6/36 cells was very inefficient and that the corresponding virus replicated poorly even in BHK-21 cells (Fig. 6 and 7). Taken together, these data suggest that the WT peptide inserted after residue 8 in nsP2 caused additional defect(s) that were not directly related to viral RNA synthesis but were harmful to the virus. In addition, we observed that although the *trans*-replicases harboring an insertion after residue 466 in nsP2 were clearly more active than replicases with an insertion after residue 618 (Fig. 1E), the opposite was true for rescued viruses: both CP expression and the number of released virus genome copies were higher for the latter mutant (Fig. 6A). At both insertion sites, viruses with wild-type nsP3 and carrying the F3A peptide in nsP2 outperformed those carrying the WT peptide, demonstrating that additional sites for Rin binding outside nsP3 were unfavorable for RNA replication in the context of viruses (Fig. 6A). Alternatively, or in addition, this outcome may indicate that binding of Rin to nsP2 inhibits other events in viral infection, such as virion formation. If this is the case, then a failure to observe such differences in transfected BHK-21 (Fig. 7A) may simply have been caused by higher transfection efficiency making (in contrast to C6/36 cells) an impact on the spread of virus infection from transfected cells to neighboring cells less noticeable.

Similar to C6/36 cells, insertion of the WT peptide after residue 8 in nsP2 failed to rescue the infectivity of 3^{F3A}CHIKV in BHK-21 cells. These data indicate that binding of G3BP to this position is not sufficient to compensate for defects caused by elimination of G3BP-binding sites from nsP3 and by the unfavorable effects resulting from the insertion of the peptide in this position. The relatively low activity of the corresponding *trans*-replicase in U2OS cells (Fig. 2D) is consistent with this hypothesis. Alternatively, this position may intrinsically be less suitable for insertion of the G3BP-binding peptide, as was also observed for WT CHIKV-based constructs harboring similar insertions (Fig. 6A and B, and Fig. 7B). Again, data about the molecular architecture of the core of alphavirus replicase are consistent with these possibilities. The N-terminal region of nsP2 was shown to form an interface between nsP2 and nsP4, located in the pore of the nsP1 ring; additionally, nsP2 is close to the tips of the hooking loops of nsP1, forming a three-way interaction network between nsP1, nsP2, and nsP4 (60). Almost certainly, such an arrangement results in steric hindrance: little room existed to accommodate large G3BP/Rin proteins bound to

the WT peptide inserted into the N terminus of nsP2. Furthermore, G3BP/Rin located in such a position is unlikely to be able to fully exhibit its proviral activities. In contrast, the C-terminal protease portion of nsP2 corresponds to an additional density located above the helicase portion of nsP2; in the proposed model, this part of nsP2 is flexible, located at a distance from nsP4 and in the vicinity of the newly revealed outer cytoplasmic ring structure likely formed by nsP3 and host proteins (60). Thus, the more distant the WT peptide insertion site is from the N terminus of nsP2, the closer G3BP/Rin bound to this site is to its natural location in the alphavirus replicase complex. Consistent with this, mutant viruses lacking G3BP-binding sites in nsP3 but harboring the WT peptide after residues 466 or 618 in nsP2 were successfully rescued in BHK-21 cells (Fig. 7A). In these cases, the infectivity of 3^{F3A}CHIKV was clearly rescued due to the ability of the inserted WT peptide to interact with G3BPs. The virus harboring the WT peptide after residue 466 was, however, unable to form functional virions, presumably because the G3BP-binding peptide inserted in this position inhibited virion formation and/or release. In contrast, virus with an insertion after residue 618 was capable of completing the full replication cycle; although greatly attenuated, its progeny successfully infected naive BHK-21 cells. The observed attenuation could plausibly be due to the repositioning of G3BP from the outer cytoplasmic ring into the core structure of replicase, which may also be suboptimal for RNA replicase activities. Furthermore, the amount of G3BP that was included in the modified replicase complex was also very likely reduced: the replicase core contains only one molecule of nsP2 (60), while the outer cytoplasmic ring structure likely contains multiple molecules of nsP3. Therefore, that infectivity of the virus was nonetheless restored was remarkable. To our knowledge, this finding represents the first demonstration of a binding site of a crucial host factor of an alphavirus being successfully moved from one replicase protein to another. Furthermore, it demonstrates that CHIKV does not truly require G3BPs to interact with nsP3, and the binding of G3BPs to nsP2 allows the infection to occur. Interestingly, all nsP2s harboring the WT peptide efficiently bound G3BP1 (Fig. 3B). Therefore, the different effects of WT peptide insertion on CHIKV RNA replication and virus rescue are unlikely to have originated from different impacts on stress granule formation. Most likely, the inserted peptides directly affected replicase complex formation and functioning as suggested above. Although nsP3 and the G3BPs bound to it are not part of the replicase core, they are part of the functional replicase complex. Our data also indicate that nsP2 and nsP3 should localize on the same side of the ring structure formed by nsP1. This provides indirect proof for the idea that nsP3 is indeed a component of the cytoplasmic ring structure that in infected cells is associated with active replication complexes (60). Additionally, if G3BP is required to protect nascent RNA strands and enable their use for the formation of new replicase complexes (36), the G3BP binding to nsP3 and the G3BP binding to nsP2 must be, at least to a degree, functionally equivalent. If G3BP mediates some other process(es) of replicase formation, for example, the interaction of replicase proteins with the RNA genome and/or other host factors, then it can perform this function when bound to nsP2.

This study broadens our understanding of virus RNA replicase-host protein interactions. Many viral proteins are known to interact with proteins of host cells, and these interactions are important, sometimes crucial, for viral infection. However, the reason (s) why these interactions are mediated via specific viral proteins is not clear. In this study, we demonstrated that a specific viral protein is not strictly needed as the interaction partner and that these interactions can, at least under certain circumstances, be mediated by other viral proteins. This ability likely leads to some consequences for viral evolution, including adaptation to new hosts that are inevitably associated with rearranged virus-host interactions. In this regard, the loss of virus-host interactions, including those crucial for virus infectivity, can be compensated for by another interaction, and the new (or restored) interaction does not necessarily need to be mediated through the original viral protein. This compensation for lost function may provide a virus with a window of opportunity for further adaptations. For example, in a short time, they can acquire second-site adaptations and eventually new binding motifs in

locations that are most suitable for meditating virus-host protein interactions, such as in long intrinsically disordered regions of replicase proteins.

MATERIALS AND METHODS

Cells and media. *Aedes albopictus*-derived C6/36 cells were maintained in Leibowitz's L-15 medium (PAN Biotech) containing 10% heat-inactivated fetal bovine serum (FBS) and 10% tryptose phosphate broth (TPB) and cultured at 28°C with no added CO_2. Human osteosarcoma (U2OS) cells (ATCC HTB-96) were maintained in Dulbecco's modified Eagle's medium (DMEM) (Corning) supplemented with 10% FBS and cultured at 37°C in a 5% CO_2 atmosphere. U2OS-derived double-null ΔΔG3BP1/2-KO cells (U2OS ΔΔ) (53) were maintained in the same medium as wild-type U2OS cells. Baby hamster kidney (BHK-21) cells (ATCC CCL-10) were maintained in Glasgow's modified Eagle's medium (GMEM) supplemented with 10% FBS, 20 mM HEPES, 10% TPB, and 1 mM L-glutamine and cultured at 37°C in a 5% CO_2 atmosphere. All media were supplemented with 100 U/mL penicillin and 0.1 mg/mL streptomycin.

Plasmids. Plasmids CMV-P1234 and Ubi-P1234 expressing wild-type P1234 of CHIKV (isolate LR2006OPY1; East/Central/South African genotype) and CMV-P1234^{GAA} and Ubi-P1234^{GAA} expressing P1234 harboring a GDD-to-GAA substitution in the active site of nsP4 have been previously described (46, 59). To obtain plasmids for the expression of polyproteins unable to bind G3BP/Rin proteins, codons for Phe479 and Phe497 in nsP3 were substituted with codons for Ala using PCR-based mutagenesis; the obtained clones were designated CMV-P123^{F3A}4 and Ubi-P123^{F3A}4. PCR-based mutagenesis was used to substitute the codon for Arg532 of nsP1 in CMV-P123^{F3A}4 to the codon of His or Gly, and the corresponding plasmids were designated CMV-P1^{R532H}23^{F3A}4 and CMV-P1^{R532G}23^{F3A}4, respectively.

DNA fragments encoding peptides with the sequence TSGGITFGDFNEGEIESLSSELLTFGDFLPGGPG (residues corresponding to amino acids 477 to 503 of WT nsP3 are underlined) or its mutant version TSGGIT**A**GDFNEGEIESLSSELLT**A**GDFLPGGPG (residues corresponding to amino acids 477 to 503 of nsP3^{F3A} are underlined, and mutated residues are in bold) were inserted into the following positions of CMV-P123^{F3A}4 and Ubi-P123^{F3A}4: (i) after codon 516 in nsP1 (site 1); (ii) after codon 8, 466, or 618 in nsP2 (sites 2a, 2b, and 2c, respectively); and (iii) after codon 612 in nsP4 (site 4). The plasmids were constructed using synthetic DNA fragments (Twist Bioscience, USA) and restriction enzyme-based cloning approaches. Plasmids containing insertions of the WT peptide sequence were designated CMV-P1^{pWT}23^{F3A}4, CMV-P12^{paWT}3^{F3A}4, CMV-P12^{pbWT}3^{F3A}4, CMV-P12^{pcWT}3^{F3A}4, CMV-P123^{F3A}4^{pWT}, Ubi-P1^{pWT}23^{F3A}4, Ubi-P12^{paWT}3^{F3A}4, Ubi-P12^{pbWT}3^{F3A}4, Ubi-P12^{pcWT}3^{F3A}4, and Ubi-P123^{F3A}4^{pWT}. Plasmids containing insertions of the F3A peptide sequences were designated CMV-P1^{pF3A}23^{F3A}4, CMV-P12^{paF3A}3^{F3A}4, CMV-P12^{pbF3A}3^{F3A}4, CMV-P12^{pcF3A}3^{F3A}4, CMV-P123^{F3A}4^{pF3A}, Ubi-P1^{pF3A}23^{F3A}4, Ubi-P12^{paF3A}3^{F3A}4, Ubi-P12^{pbF3A}3^{F3A}4, Ubi-P12^{pcF3A}3^{F3A}4, and Ubi-P123^{F3A}4^{pF3A}. In addition, a DNA fragment encoding a flexible 10GS linker with the sequence GSGSGSGSGS was inserted into CMV-P123^{F3A}4 after codon 466 of nsP2 (site 2b); the obtained plasmid was designated CMV-P12^{pb10GS}3^{F3A}4.

The icDNA clones were based on previously described clones SP6-ICRES1 (63) and SP6-CHIKV F3A$_{NC}$ (42) and are named SP6-CHIKV and SP6-3^{F3A}CHIKV, respectively, in this study. icDNAs containing inserts encoding WT or F3A peptide in the previously mentioned sites in nsP2 were assembled from SP6-CHIKV or SP6-3^{F3A}CHIKV and synthetic DNAs (Twist Bioscience, USA) using restriction enzyme-based cloning approaches. The obtained clones were designated SP6-CHIKV^{2paWT}, SP6-CHIKV^{2paF3A}, SP6-3^{F3A}CHIKV^{2paWT}, SP6-3^{F3A}CHIKV^{2paF3A}, SP6-CHIKV^{2pbWT}, SP6-CHIKV^{2pbF3A}, SP6-3^{F3A}CHIKV^{2pbWT}, SP6-3^{F3A}CHIKV^{2pbF3A}, SP6-CHIKV^{2pcWT}, SP6-CHIKV^{2pcF3A}, SP6-3^{F3A}CHIKV^{2pcWT}, and SP6-3^{F3A}CHIKV^{2pcF3A}.

The CMV-EGFP-HVD plasmid used for the expression of EGFP fused with the HVD in CHIKV nsP3 has been previously described (32). To obtain plasmids expressing nsP2 or its mutant forms, the sequence encoding the HVD of nsP3 was replaced with a sequence encoding nsP2 from CMV-P1234, CMV-P12^{paWT}3^{F3A}4, CMV-P12^{paF3A}3^{F3A}4, CMV-P12^{pbWT}3^{F3A}4, CMV-P12^{pbF3A}3^{F3A}4, CMV-P12^{pb10GS}3^{F3A}4, CMV-P12^{pcWT}3^{F3A}4, or CMV-P12^{pcF3A}3^{F3A}4 using PCR amplification and restriction enzyme-based cloning approaches. The obtained plasmids were designated CMV-EGFP-nsP2, CMV-EGFP-nsP2^{paWT}, CMV-EGFP-nsP2^{paF3A}, CMV-EGFP-nsP2^{pbWT}, CMV-EGFP-nsP2^{pbF3A}, CMV-EGFP-nsP2^{pb10GS}, CMV-EGFP-nsP2^{pcWT}, and CMV-EGFP-nsP2^{pcF3A}. To express these proteins in C6/36 mosquito cells, sequences encoding EGFP-HVD and EGFP-nsP2 fusion proteins were inserted into the expression vector between the *Aedes aegypti* polyubiquitin promoter and the simian virus 40 late polyadenylation region; the obtained plasmids were designated Ubi-EGFP-HVD, Ubi-EGFP-nsP2, Ubi-EGFP-nsP2^{paWT}, Ubi-EGFP-nsP2^{paF3A}, Ubi-EGFP-nsP2^{pbWT}, Ubi-EGFP-nsP2^{pbF3A}, Ubi-EGFP-nsP2^{pb10GS}, Ubi-EGFP-nsP2^{pcWT}, and Ubi-EGFP-nsP2^{pcF3A}. The sequence encoding *Aedes albopictus* Rin was codon optimized for expression in *Aedes albopictus* cells, and its 3′ end was fused with a sequence encoding a flexible linker and a V5 epitope tag. The cassette was obtained as synthetic DNA (Genscript, USA) and cloned as described above; the obtained plasmid was designated Ubi-AlbRin-V5. The sequences of all plasmids encoding CHIKV proteins (Table 1) were verified using Sanger sequencing and are available from the authors upon request.

***Trans*-replication assay.** The *trans*-replication assay was performed using human (HSPolI-Fluc-Gluc) and *Aedes albopictus* (AlbPolI-Fluc-Gluc) RNA polymerase I promoter-based plasmids for the production of an RNA template for the CHIKV replicase (45). Briefly, C6/36 cells grown in 12-well plates to ~80% confluence were cotransfected with 0.5 μg of Ubi-P1234 (or its mutant variants) and 0.5 μg of AlbPolI-Fluc-Gluc using Lipofectamine LTX with PLUS reagent (Thermo Fisher Scientific) according to the manufacturer's instructions and incubated at 28°C for 48 h. Wild-type U2OS and U2OS ΔΔ cells grown in 12-well plates to ~80% confluence were cotransfected with 1 μg of CMV-P1234 (or its mutant variants) and 1 μg of HSPolI-Fluc-Gluc using Lipofectamine LTX with PLUS reagent and incubated at 37°C for 18 h. In some experiments with U2OS ΔΔ cells, 1 μg of CMV-G3BP1 plasmid (53) was added to the transfection

TABLE 1 Names of the plasmids used in the experiments

Plasmid	Location of the inserted WT peptide[a]			
	nsP1	nsP2	nsP4	nsP3[e]
CMV/Ubi-P1234				WT[b]
CMV/Ubi-P123^{F3A}4				A479 and A497
CMV-P1^{R532H}23^{F3A}4				A479 and A497
CMV-P1^{R532G}23^{F3A}4				A479 and A497
CMV/Ubi-P1^{pWT}23^{F3A}4	Site 1[c]			A479 and A497
CMV/Ubi-P12^{paWT}3^{F3A}4		Site 2a[c]		A479 and A497
CMV/Ubi-P12^{pbWT}3^{F3A}4		Site 2b[c]		A479 and A497
CMV/Ubi-P12^{pcWT}3^{F3A}4		Site 2c[c]		A479 and A497
CMV/Ubi-P123^{F3A}4^{pWT}			Site 4[c]	A479 and A497
SP6-3^{F3A}CHIKV^{2paWT}		Site 2a		A479 and A497
SP6-3^{F3A}CHIKV^{2pbWT}		Site 2b		A479 and A497
SP6-3^{F3A}CHIKV^{2pcWT}		Site 2c		A479 and A497
SP6-CHIKV^{2paWT}		Site 2a		WT
SP6-CHIKV^{2pbWT}		Site 2b		WT
SP6-CHIKV^{2pcWT}		Site 2c		WT
SP6-CHIKV				WT
SP6-3^{F3A}CHIKV				A479 and A497
CMV/Ubi-EGFP-nsP2^{paWT}		Site 2a		NA
CMV/Ubi-EGFP-nsP2^{pbWT}		Site 2b		NA
CMV/Ubi-EGFP-nsP2^{pcWT}		Site 2c		NA
Location of inserted F3A peptide[a]				
CMV/Ubi-P1^{pF3A}23^{F3A}4	Site 1			A479 and A497
CMV/Ubi-P12^{paF3A}3^{F3A}4		Site 2a		A479 and A497
CMV/Ubi-P12^{pbF3A}3^{F3A}4		Site 2b		A479 and A497
CMV/Ubi-P12^{pcF3A}3^{F3A}4		Site 2c		A479 and A497
CMV/Ubi-P123^{F3A}4^{pF3A}			Site 4	A479 and A497
SP6-3^{F3A}CHIKV^{2paF3A}		Site 2a		A479 and A497
SP6-3^{F3A}CHIKV^{2pbF3A}		Site 2b		A479 and A497
SP6-3^{F3A}CHIKV^{2pcF3A}		Site 2c		A479 and A497
SP6-CHIKV^{2paF3A}		Site 2a		WT
SP6-CHIKV^{2pbF3A}		Site 2b		WT
SP6-CHIKV^{2pcF3A}		Site 2c		WT
CMV/Ubi-EGFP-nsP2^{paF3A}		Site 2a		NA
CMV/Ubi-EGFP-nsP2^{pbF3A}		Site 2b		NA
CMV/Ubi-EGFP-nsP2^{pcF3A}		Site 2c		NA
Location of inserted 10GS linker[d]				
CMV-P12^{pb10GS}3^{F3A}4		Site 2b		A479 and A497
CMV/Ubi-EGFP-nsP2^{pb10GS}		Site 2b		NA

[a]The WT peptide contains amino acid residues 477 to 503 of CHIKV nsP3 (ITFGDFNEGEIESLSSELLTFGDFLPG); F3A peptide has sequence IT**A**GDFNEGEIESLSSELLT**A**GDFLPG (mutated residues in bold).
[b]F479 and F497.
[c]Site 1: after codon 516 in nsP1; site 2a: after codon 8 in nsP2; site 2b: after codon 466 in nsP2; site 2c: after codon 618 in nsP2; site 4: after codon 612 in nsP4.
[d]The 10GS linker has sequence GSGSGSGSGS.
[e]NA, not applicable.

mixture. After incubation, the cells were lysed with lysis buffer (Promega), and Fluc and Gluc activities were measured using a dual-luciferase reporter kit and GloMAX SIS luminometer (Promega). All Fluc and Gluc activities were normalized to those obtained with control cells cotransfected with CMV-P1234^{GAA} (human) or Ubi-P1234^{GAA} (mosquito) and the corresponding plasmid expressing the RNA template. All experiments were repeated at least three times.

Virus rescue, titration, and propagation. Plasmids containing icDNA of wild-type CHIKV or its mutants were linearized by NotI digestion and purified using a DNA Clean & Concentrator-5 kit (Zymo Research). Linearized cDNA (100 ng) was transcribed *in vitro* using the mMACHINE SP6 transcription kit (Ambion); 5 μg of the obtained transcripts was used to transfect C6/36 or BHK-21 cells using Lipofectamine 2000 reagent (Thermo Fisher Scientific) according to the manufacturer's instructions. The transfected C6/36 cells were incubated at 28°C for 72 h; BHK-21 cells were incubated at 37°C until CPEs were observed or for 72 h. At these times, P_0 virus stocks were harvested. Then, 150 μL of each obtained P_0 stock was used to infect 1×10^6 BHK-21 cells grown in 6-well cell culture plates. After 1 h of incubation with virus, inoculum was replaced with GMEM containing 2% FBS, and the cells were incubated at 37°C until CPEs were observed or for 72 h. At these times, P_1 virus stocks were harvested.

TABLE 2 Sequences of the primers used in the experiments

Primer	Sequence	Amplified region of CHIKV genome (nucleotide residues)
Set1F	5′-ATTCTGCTTACACACAGACGTCTCATG-3′	396–593
Set1R	5′-TTTGTCGAGTATGAGGGGTAGGCACC-3′	
Set2F	5′-TGCTATTTGACCACAACGTG-3′	4925–6194
Set2R	5′-GCTGCTGCCAGTACATTCTG-3′	
Set3F	5′-GACCTGATCCCATACAGCGG-3′	1435–2179
Set3R	5′-TGCCAGATCCCGGTACTCCG-3′	

Western blot analysis. Cells used to produce P_0 and P_1 stocks were harvested when the viral stocks were collected. To obtain samples from mosquito and human cells expressing CHIKV P1234 or its mutant variants, ~2 × 10^6 U2OS or ~1.6 × 10^7 C6/36 cells grown on 6-well cell culture plates were transfected with 5 μg of CMV-P1234 or Ubi-P1234 (or their mutant variants), respectively, using Lipofectamine LTX with PLUS reagent. U2OS cells were incubated at 37°C for 18 h, while C6/36 cells were incubated at 28°C for 48 h. After incubation, the cells were washed with phosphate-buffered saline (PBS), collected, lysed by boiling in Laemmli sample buffer for 5 min, and subjected to SDS-PAGE in 10% or 12% gels. The separated proteins were transferred to polyvinylidene difluoride membranes and visualized using antibodies against CHIKV nsP1, nsP2, nsP3, or CP (all produced in-house). An antibody against β-actin (sc-47778; Santa Cruz Biotechnology) was used to detect the loading control. Membranes were washed 3 times with PBS, incubated with the corresponding secondary antibodies conjugated to fluorescent labels (Li-Cor), washed, and imaged using a Li-Cor Odyssey Fc imaging system.

Pulldown assay. Approximately 2 × 10^6 U2OS cells grown on 60-mm cell culture dishes were transfected with 5 μg of CMV-EGFP-HVD, CMV-EGFP-nsP2, CMV-EGFP-nsP2^{paWT}, CMV-EGFP-nsP2^{paF3A}, CMV-EGFP-nsP2^{pbWT}, CMV-EGFP-nsP2^{pbF3A}, CMV-EGFP-nsP2^{pb10GC}, CMV-EGFP-nsP2^{pcWT}, or CMV-EGFP-nsP2^{pcF3A} using Lipofectamine LTX with PLUS reagent. Alternatively, approximately 1.6 × 10^7 C6/36 cells were grown on two 60-mm cell culture dishes, and each dish was cotransfected with 5 μg of Ubi-AlbRin-V5 and 5 μg of Ubi-EGFP-HVD, Ubi-EGFP-nsP2, Ubi-EGFP-nsP2^{paWT}, Ubi-EGFP-nsP2^{paF3A}, Ubi-EGFP-nsP2^{pbWT}, Ubi-EGFP-nsP2^{pbF3A}, Ubi-EGFP-nsP2^{pb10GC}, Ubi-EGFP-nsP2^{pcWT}, or Ubi-EGFP-nsP2^{pcF3A} using Lipofectamine LTX with PLUS reagent. At 48 h posttransfection (hpt), the cells were collected and washed with PBS, and host proteins bound to EGFP-HDV or EGFP-nsP2 fusion proteins were pulled down as described previously (32). Briefly, cells were lysed using 700 μL of cold lysis buffer (20 mM HEPES, pH 7.2; 150 mM NaCl; 2 mM $MgCl_2$; 100 mM K-acetate; 1% Triton X-100; 0.1% Tween 20; and 1 tablet of Pierce protease inhibitor [Thermo Fisher Scientific] per 50 mL of lysis buffer). After lysing on ice for 30 min, cell debris was removed by centrifugation at 15,000 × *g* for 10 min at 4°C. The supernatant was transferred to a clean tube and incubated with EGFP-binding magnetic beads (GFP-trap M, ChromoTek) for 1 h at 4°C. After incubation, the beads were washed four times with lysis buffer, and bound proteins were denatured by boiling in Laemmli sample buffer for 5 min. The obtained samples were used for immunoblot analysis as described above; antibodies against G3BP1 (sc-365338) were from Santa Cruz Biotechnology, and antibodies against the V5 epitope tag (ab27671) were from Abcam, Inc.

RT-qPCR and RT-PCR and sequencing. Aliquots (200 μL) of stock harvested from C6/36 and BHK-21 cells were used for isolation of CHIKV genomic RNA. RNA was purified using a Quick-RNA miniprep kit (Zymo Research) according to the manufacturer's protocol and eluted in 20 μL of RNase-free water. One-half of the obtained RNA was used for the synthesis of cDNA with a First Strand cDNA synthesis kit and random primers (Thermo Fisher Scientific); the reaction was conducted in a 20-μL volume. Genome copy numbers of wild-type and mutant viruses were determined by RT-qPCR using a LightCycler 480 II instrument (Roche) as described previously (20). Briefly, the reaction was performed in a 10-μL volume on a 384-well white plate. The mixture contained 1 × HOT FIREPol EvaGreen qPCR Mix Plus (no ROX) (Solis BioDyne, Estonia), 200 nM primers (Set1F and Set1R; Table 2), and 6 μL of the previously mentioned cDNAs. Each sample was analyzed using three technical repeats; nuclease-free water was used as the negative control. The qPCR program was as follows: 95°C for 12 min and 50 cycles of 95°C for 15 s, 63°C for 30 s, and 72°C for 30 s. A melting curve analysis was performed to exclude the influence of primer dimers.

Regions covering the HVD in nsP3 and the region containing the 1/2 site were amplified using the corresponding primers (Set2F and Set2R or Set3F and Set3R, Table 2), DreamTaq DNA polymerase (Thermo Fisher Scientific), and the cDNAs described above. The obtained PCR products were purified using a DNA Clean & Concentrator kit (Zymo Research) and cloned using a cloneJET PCR cloning kit (Thermo Fisher Scientific) according to the manufacturer's protocol. For each of the obtained fragments, 5 clones were randomly selected, the corresponding plasmids were purified, and the cloned fragments were analyzed using Sanger sequencing.

Indirect immunofluorescence microscopy. U2OS cells grown on coverslips were transfected with CMV-EGFP-nsP2, CMV-EGFP-nsP2^{pcWT}, or CMV-EGFP-nsP2^{pcF3A}. At 24 hpt, the cells were fixed with 4% paraformaldehyde in PBS, permeabilized with 0.5% Triton X-100 in PBS, and blocked with 5% FBS in PBS. nsP2 was visualized using rabbit anti-CHIKV nsP2 antibody (arisen against the helicase portion of nsP2, amino acid residues 1 to 470), mouse anti-G3BP1 antibody was used to detect G3BP1, and secondary antibodies were conjugated with Alexa 488 or Alexa 568. The images were acquired using a Zeiss LSM 710 confocal microscope.

Statistical analysis. GraphPad Prism software (version 5.01) was used to perform statistical analysis. The data were analyzed by Student's unpaired one-tailed *t* test.

Data availability. All data used to reach the conclusions in the submitted paper and any data required to replicate the study findings are presented in the manuscript; raw data are available from the

authors upon request. All plasmids encoding CHIKV proteins are listed in the Table 1. Their sequences are available from the authors upon request. All plasmids used in the study are available from the authors without restrictions.

ACKNOWLEDGMENTS

This work was supported by the European Regional Development Fund through the Centre of Excellence in Molecular Cell Engineering, Estonia, 2014-2020.4.01.15-013, by basic funding from the Institute of Technology, and by an Estonian Research Council grant (PRG1154). The funders played no role in the study design, data collection, or interpretation or in the decision to submit the work for publication.

We thank Margus Varjak for his help with confocal microscopy.

REFERENCES

1. Silva LA, Dermody TS. 2017. Chikungunya virus: Epidemiology, replication, disease mechanisms, and prospective intervention strategies. J Clin Invest 127:737–749. https://doi.org/10.1172/JCI84417.
2. Strauss JH, Strauss EG. 1994. The alphaviruses: gene expression, replication, and evolution. Microbiol Rev 58:491–562. https://doi.org/10.1128/mr.58.3.491-562.1994.
3. Firth AE, Chung BY, Fleeton MN, Atkins JF. 2008. Discovery of frameshifting in Alphavirus 6K resolves a 20-year enigma. Virol J 5:108. https://doi.org/10.1186/1743-422X-5-108.
4. Ahola T, McInerney G, Merits A. 2021. Alphavirus RNA replication in vertebrate cells. Adv Virus Res 111:111–156. https://doi.org/10.1016/bs.aivir.2021.07.003.
5. Rubach JK, Wasik BR, Rupp JC, Kuhn RJ, Hardy RW, Smith JL. 2009. Characterization of purified Sindbis virus nsP4 RNA-dependent RNA polymerase activity in vitro. Virology 384:201–208. https://doi.org/10.1016/j.virol.2008.10.030.
6. Bia Tan Y, Lello LS, Liu X, Law Y-S, Kang C, Lescar J, Zheng J, Merits A, Luo D. 2021. A crystal structure of alphavirus nonstructural protein 4 (nsP4) reveals an intrinsically dynamic RNA-dependent RNA polymerase. bioRxiv https://doi.org/10.1101/2021.05.27.445971.
7. Chen MW, Tan YB, Zheng J, Zhao Y, Lim BT, Cornvik T, Lescar J, Ng LFP, Luo D. 2017. Chikungunya virus nsP4 RNA-dependent RNA polymerase core domain displays detergent-sensitive primer extension and terminal adenylyltransferase activities. Antiviral Res 143:38–47. https://doi.org/10.1016/j.antiviral.2017.04.001.
8. Ahola T, Laakkonen P, Vihinen H, Kääriäinen L. 1997. Critical residues of Semliki Forest virus RNA capping enzyme involved in methyltransferase and guanylyltransferase-like activities. J Virol 71:392–397. https://doi.org/10.1128/JVI.71.1.392-397.1997.
9. Zhang K, Law YS, Law MCY, Tan YB, Wirawan M, Luo D. 2021. Structural insights into viral RNA capping and plasma membrane targeting by Chikungunya virus nonstructural protein 1. Cell Host Microbe 29:757–764.e3. https://doi.org/10.1016/j.chom.2021.02.018.
10. Jones R, Bragagnolo G, Arranz R, Reguera J. 2021. Capping pores of alphavirus nsP1 gate membranous viral replication factories. Nature 589:615–619. https://doi.org/10.1038/s41586-020-3036-8.
11. Das PK, Merits A, Lulla A. 2014. Functional cross-talk between distant domains of chikungunya virus non-structural protein 2 is decisive for its RNA-modulating activity. J Biol Chem 289:5635–5653. https://doi.org/10.1074/jbc.M113.503433.
12. Rikkonen M, Peränen J, Kääriäinen L. 1994. ATPase and GTPase activities associated with Semliki Forest virus nonstructural protein nsP2. J Virol 68:5804–5810. https://doi.org/10.1128/JVI.68.9.5804-5810.1994.
13. Vasiljeva L, Merits A, Auvinen P, Kääriäinen L. 2000. Identification of a novel function of the Alphavirus capping apparatus. RNA 5′-triphosphatase activity of Nsp2. J Biol Chem 275:17281–17287. https://doi.org/10.1074/jbc.M910340199.
14. Gomez de Cedrón M, Ehsani N, Mikkola ML, García JA, Kääriäinen L. 1999. RNA helicase activity of Semliki Forest virus replicase protein NSP2. FEBS Lett 448:19–22. https://doi.org/10.1016/S0014-5793(99)00321-X.
15. Law YS, Utt A, Tan YB, Zheng J, Wang S, Chen MW, Griffin PR, Merits A, Luo D. 2019. Structural insights into RNA recognition by the Chikungunya virus nsP2 helicase. Proc Natl Acad Sci U S A 116:9558–9567. https://doi.org/10.1073/pnas.1900656116.
16. Russo AT, White MA, Watowich SJ. 2006. The crystal structure of the Venezuelan equine encephalitis alphavirus nsP2 protease. Structure 14:1449–1458. https://doi.org/10.1016/j.str.2006.07.010.
17. Rausalu K, Utt A, Quirin T, Varghese FS, Žusinaite E, Das PK, Ahola T, Merits A. 2016. Chikungunya virus infectivity, RNA replication and non-structural polyprotein processing depend on the nsP2 protease's active site cysteine residue. Sci Rep 6:37124. https://doi.org/10.1038/srep37124.
18. Sawicki DL, Sawicki SG. 1980. Short-lived minus-strand polymerase for Semliki Forest virus. J Virol 34:108–118. https://doi.org/10.1128/JVI.34.1.108-118.1980.
19. Lemm A, Rümenapf T, Strauss EG, Strauss JH, Rice CM. 1994. Polypeptide requirements for assembly of functional Sindbis virus replication complexes: a model for the temporal regulation of minus- and plus-strand RNA synthesis. EMBO J 13:2925–2934. https://doi.org/10.1002/j.1460-2075.1994.tb06587.x.
20. Law Y-S, Wang S, Tan YB, Shih O, Utt A, Goh WY, Lian B-J, Chen MW, Jeng U-S, Merits A, Luo D. 2021. Interdomain flexibility of chikungunya virus nsP2 helicase-protease differentially influences viral RNA replication and infectivity. J Virol 95:e01470-20. https://doi.org/10.1128/JVI.01470-20.
21. Shin G, Yost SA, Miller MT, Elrod EJ, Grakoui A, Marcotrigiano J. 2012. Structural and functional insights into alphavirus polyprotein processing and pathogenesis. Proc Natl Acad Sci U S A 109:16534–16539. https://doi.org/10.1073/pnas.1210418109.
22. Meshram CD, Agback P, Shiliaev N, Urakova N, Mobley JA, Agback T, Frolova EI, Frolov I. 2018. Multiple host factors interact with the hypervariable domain of chikungunya virus nsP3 and determine viral replication in cell-specific mode. J Virol 92:e00838-18. https://doi.org/10.1128/JVI.00838-18.
23. Malet H, Coutard B, Jamal S, Dutartre H, Papageorgiou N, Neuvonen M, Ahola T, Forrester N, Gould EA, Lafitte D, Ferron F, Lescar J, Gorbalenya AE, de Lamballerie X, Canard B. 2009. The crystal structures of chikungunya and Venezuelan equine encephalitis virus nsP3 macro domains define a conserved adenosine binding pocket. J Virol 83:6534–6545. https://doi.org/10.1128/JVI.00189-09.
24. McPherson RL, Abraham R, Sreekumar E, Ong SE, Cheng SJ, Baxter VK, Kistemaker HAV, Filippov DV, Griffin DE, Leung AKL. 2017. ADP-ribosylhydrolase activity of Chikungunya virus macrodomain is critical for virus replication and virulence. Proc Natl Acad Sci U S A 114:1666–1671. https://doi.org/10.1073/pnas.1621485114.
25. Abraham R, Hauer D, McPherson RL, Utt A, Kirby IT, Cohen MS, Merits A, Leung AKL, Griffin DE. 2018. ADP-ribosyl-binding and hydrolase activities of the alphavirus nsP3 macrodomain are critical for initiation of virus replication. Proc Natl Acad Sci U S A 115:E10457–E10466. https://doi.org/10.1073/pnas.1812130115.
26. Abraham R, McPherson RL, Dasovich M, Badiee M, Leung AKL, Griffin DE. 2020. Both ADP-ribosyl-binding and hydrolase activities of the alphavirus nsp3 macrodomain affect neurovirulence in mice. mBio 11:e03253-19. https://doi.org/10.1128/mBio.03253-19.
27. Jayabalan AK, Adivarahan S, Koppula A, Abraham R, Batish M, Zenklusen D, Griffin DE, Leung AKL. 2021. Stress granule formation, disassembly, and composition are regulated by alphavirus ADP-ribosylhydrolase activity. Proc Natl Acad Sci U S A 115:e2021719118. https://doi.org/10.1073/pnas.2021719118.
28. Gao Y, Goonawardane N, Ward J, Tuplin A, Harris M. 2019. Multiple roles of the non-structural protein 3 (nsP3) alphavirus unique domain (AUD) during Chikungunya virus genome replication and transcription. PLoS Pathog 15:e1007239. https://doi.org/10.1371/journal.ppat.1007239.
29. Dominguez F, Shiliaev N, Lukash T, Agback P, Palchevska O, Gould JR, Meshram CD, Prevelige PE, Green TJ, Agback T, Frolova EI, Frolov I. 2021. NAP1L1 and NAP1L4 binding to hypervariable domain of chikungunya virus nsP3 protein is bivalent and requires phosphorylation. J Virol 95:e00836-21. https://doi.org/10.1128/JVI.00836-21.

30. Lukash T, Agback T, Dominguez F, Shiliaev N, Meshram C, Frolova EI, Agback P, Frolov I. 2020. Structural and functional characterization of host FHL1 protein interaction with hypervariable domain of chikungunya virus nsP3 protein. J Virol 95:e01672-20. https://doi.org/10.1128/JVI.01672-20.
31. Agback P, Dominguez F, Pustovalova Y, Lukash T, Shiliaev N, Orekhov VY, Frolov I, Agback T, Frolova EI. 2019. Structural characterization and biological function of bivalent binding of CD2AP to intrinsically disordered domain of chikungunya virus nsP3 protein. Virology 537:130–142. https://doi.org/10.1016/j.virol.2019.08.022.
32. Mutso M, Morro AM, Smedberg C, Kasvandik S, Aquilimeba M, Teppor M, Tarve L, Lulla A, Lulla V, Saul S, Thaa B, McInerney G, Merits A, Varjak M. 2018. Mutation of CD2AP and SH3KBP1 binding motif in alphavirus nsP3 hypervariable domain results in attenuated virus. Viruses 10:226. https://doi.org/10.3390/v10050226.
33. Teppor M, Žusinaite E, Merits A. 2021. Phosphorylation sites in the hypervariable domain in chikungunya virus nsP3 are crucial for viral replication. J Virol 95:e02276-20. https://doi.org/10.1128/JVI.02276-20.
34. Vihinen H, Saarinen J. 2000. Phosphorylation site analysis of Semliki Forest virus nonstructural protein 3. J Biol Chem 275:7775–7783. https://doi.org/10.1074/jbc.M002195200.
35. Li G, La Starza MW, Reef Hardy W, Strauss JH, Rice CM. 1990. Phosphorylation of Sindbis virus nsP3 in vivo and in vitro. Virology 179:416–427. https://doi.org/10.1016/0042-6822(90)90310-N.
36. Kim DY, Reynaud JM, Rasalouskaya A, Akhrymuk I, Mobley JA, Frolov I, Frolova EI. 2016. New World and Old World alphaviruses have evolved to exploit different components of stress granules, FXR and G3BP proteins, for assembly of viral replication complexes. PLoS Pathog 12:e1005810. https://doi.org/10.1371/journal.ppat.1005810.
37. Kristensen O. 2015. Crystal structure of the G3BP2 NTF2-like domain in complex with a canonical FGDF motif peptide. Biochem Biophys Res Commun 467:53–57. https://doi.org/10.1016/j.bbrc.2015.09.123.
38. Fros JJ, Geertsema C, Zouache K, Baggen J, Domeradzka N, Van Leeuwen DM, Flipse J, Vlak JM, Failloux AB, Pijlman GP. 2015. Mosquito Rasputin interacts with chikungunya virus nsP3 and determines the infection rate in Aedes albopictus. Parasites Vectors 8:464. https://doi.org/10.1186/s13071-015-1070-4.
39. Fros JJ, Domeradzka NE, Baggen J, Geertsema C, Flipse J, Vlak JM, Pijlman GP. 2012. Chikungunya virus nsP3 blocks stress granule assembly by recruitment of G3BP into cytoplasmic foci. J Virol 86:10873–10879. https://doi.org/10.1128/JVI.01506-12.
40. Panas MD, Varjak M, Lulla A, Eng KE, Merits A, Hedestam GBK, McInerney GM. 2012. Sequestration of G3BP coupled with efficient translation inhibits stress granules in Semliki Forest virus infection. Mol Biol Cell 23:4701–4712. https://doi.org/10.1091/mbc.E12-08-0619.
41. Göertz GP, Lingemann M, Geertsema C, Abma-Henkens MHC, Vogels CBF, Koenraadt CJM, van Oers MM, Pijlman GP. 2018. Conserved motifs in the hypervariable domain of chikungunya virus nsP3 required for transmission by Aedes aegypti mosquitoes. PLoS Negl Trop Dis 12:e0006958. https://doi.org/10.1371/journal.pntd.0006958.
42. Götte B, Utt A, Fragkoudis R, Merits A, McInerney GM. 2020. Sensitivity of alphaviruses to G3BP deletion correlates with efficiency of replicase polyprotein processing. J Virol 94:e01681-19. https://doi.org/10.1128/JVI.01681-19.
43. Schulte T, Liu L, Panas MD, Thaa B, Dickson N, Götte B, Achour A, McInerney GM. 2016. Combined structural, biochemical and cellular evidence demonstrates that both FGDF motifs in alphavirus nsp3 are required for efficient replication. Open Biol 6:160078. https://doi.org/10.1098/rsob.160078.
44. Kendall C, Khalid H, Müller M, Banda DH, Kohl A, Merits A, Stonehouse NJ, Tuplin A. 2019. Structural and phenotypic analysis of Chikungunya virus RNA replication elements. Nucleic Acids Res 47:9296–9312. https://doi.org/10.1093/nar/gkz640.
45. Utt A, Rausalu K, Jakobson M, Männik A, Alphey L, Fragkoudis R, Merits A. 2019. Design and use of chikungunya virus replication templates utilizing mammalian and mosquito RNA polymerase I-mediated transcription. J Virol 93:e00794-19. https://doi.org/10.1128/JVI.00794-19.
46. Utt A, Quirin T, Saul S, Hellström K, Ahola T, Merits A. 2016. Versatile trans-replication systems for chikungunya virus allow functional analysis and tagging of every replicase protein. PLoS One 11:e0151616. https://doi.org/10.1371/journal.pone.0151616.
47. Atasheva S, Gorchakov R, English R, Frolov I, Frolova E. 2007. Development of Sindbis viruses encoding nsP2/GFP chimeric proteins and their application for studying nsP2 functioning. J Virol 81:5046–5057. https://doi.org/10.1128/JVI.02746-06.
48. Lulla V, Karo-Astover L, Rausalu K, Saul S, Merits A, Lulla A. 2018. Timeliness of proteolytic events is prerequisite for efficient functioning of the alphaviral replicase. J Virol 92:e1008825. https://doi.org/10.1128/JVI.00151-18.
49. Lello LS, Utt A, Bartholomeeusen K, Wang S, Rausalu K, Kendall C, Coppens S, Fragkoudis R, Tuplin A, Alphey L, Ariën KK, Merits A. 2020. Cross-utilisation of template RNAs by alphavirus replicases. PLoS Pathog 16:e1008825. https://doi.org/10.1371/journal.ppat.1008825.
50. Vasiljeva L, Valmu L, Kääriäinen L, Merits A. 2001. Site-specific protease activity of the carboxyl-terminal domain of Semliki Forest virus replicase protein nsP2. J Biol Chem 276:30786–30793. https://doi.org/10.1074/jbc.M104786200.
51. Scholte FEM, Tas A, Albulescu IC, Žusinaite E, Merits A, Snijder EJ, van Hemert MJ. 2015. Stress granule components G3BP1 and G3BP2 play a proviral role early in Chikungunya virus replication. J Virol 89:4457–4469. https://doi.org/10.1128/JVI.03612-14.
52. Aguilera-Gomez A, Zacharogianni M, van Oorschot MM, Genau H, Grond R, Veenendaal T, Sinsimer KS, Gavis EA, Behrends C, Rabouille C. 2017. Phospho-Rasputin stabilization by Sec16 is required for stress granule formation upon amino acid starvation. Cell Rep 20:935–948. https://doi.org/10.1016/j.celrep.2017.06.042.
53. Kedersha N, Panas MD, Achorn CA, Lyons S, Tisdale S, Hickman T, Thomas M, Lieberman J, McInerney GM, Ivanov P, Anderson P. 2016. G3BP-Caprin1-USP10 complexes mediate stress granule condensation and associate with 40S subunits. J Cell Biol 212:845–860. https://doi.org/10.1083/jcb.201508028.
54. Matsuki H, Takahashi M, Higuchi M, Makokha GN, Oie M, Fujii M. 2013. Both G3BP1 and G3BP2 contribute to stress granule formation. Genes Cells 18:135–146. https://doi.org/10.1111/gtc.12023.
55. Kedersha N, Anderson P. 2002. Stress granules: sites of mRNA triage that regulate mRNA stability and translatability. Biochem Soc Trans 30:963–969. https://doi.org/10.1042/bst0300963.
56. Cristea IM, Rozjabek H, Molloy KR, Karki S, White LL, Rice CM, Rout MP, Chait BT, MacDonald MR. 2010. Host factors associated with the Sindbis virus RNA-dependent RNA polymerase: role for G3BP1 and G3BP2 in virus replication. J Virol 84:6720–6732. https://doi.org/10.1128/JVI.01983-09.
57. Varjak M, Saul S, Arike L, Lulla A, Peil L, Merits A. 2013. Magnetic fractionation and proteomic dissection of cellular organelles occupied by the late replication complexes of Semliki Forest virus. J Virol 87:10295–10312. https://doi.org/10.1128/JVI.01105-13.
58. Götte B, Panas MD, Hellström K, Liu L, Samreen B, Larsson O, Ahola T, McInerney GM. 2019. Separate domains of G3BP promote efficient clustering of alphavirus replication complexes and recruitment of the translation initiation machinery. PLoS Pathog 15:e1007842. https://doi.org/10.1371/journal.ppat.1007842.
59. Bartholomeeusen K, Utt A, Coppens S, Rausalu K, Vereecken K, Ariën KK, Merits A. 2018. A chikungunya virus trans -replicase system reveals the importance of delayed nonstructural polyprotein processing for efficient replication complex formation in mosquito cells. J Virol 92:e00152-18. https://doi.org/10.1128/JVI.00152-18.
60. Tan YB, Chmielewski D, Law MCY, Zhang K, He Y, Chen M, Jin J, Luo D, Chiu W. 2022. Molecular architecture of the chikungunya virus replication complex. bioRxiv https://doi.org/10.1101/2022.04.08.487651.
61. Sólyom Z, Ma P, Schwarten M, Bosco M, Polidori A, Durand G, Willbold D, Brutscher B. 2015. The disordered region of the HCV protein NS5A: conformational dynamics, SH3 binding, and phosphorylation. Biophys J 109:1483–1496. https://doi.org/10.1016/j.bpj.2015.06.040.
62. Lello LS, Bartholomeeusen K, Wang S, Coppens S, Fragkoudis R, Alphey L, Ariën KK, Merits A, Utt A. 2021. nsP4 is a major determinant of alphavirus replicase activity and template selectivity. J Virol 95:e00355-21. https://doi.org/10.1128/JVI.00355-21.
63. Pohjala L, Utt A, Varjak M, Lulla A, Merits A, Ahola T, Tammela P. 2011. Inhibitors of alphavirus entry and replication identified with a stable Chikungunya replicon cell line and virus-based assays. PLoS One 6:e28923. https://doi.org/10.1371/journal.pone.0028923.